OFFICE OF ENVIRONMENTAL HEALTH HAZARD ASSESSMENT

Air Toxics Hot Spots Program

Acrolein

Cancer Inhalation Unit Risk Factor

Technical Support Document for
Cancer Potency Factors
Appendix B

Public Review Draft

May 2026

Air and Site Assessment and Climate Indicators Branch

Office of Environmental Health Hazard Assessment

California Environmental Protection Agency

Page Intentionally Left Blank

Acrolein

Cancer Inhalation Unit Risk Factor

Technical Support Document for Cancer Potency Factors Appendix B

Prepared by the

Office of Environmental Health Hazard Assessment

Kristina Thayer, Ph.D., Director

Project Leads, in alphabetical order

Daryn E. Dodge, Ph.D.

Ola Wasel, Ph.D., M.P.H.

Contributors, in alphabetical order

Vanessa Cheng, Ph.D.

Homa Sadeghi, Ph.D.

Rose Schmitz, M.S.

Rona M. Silva, Ph.D.

Feng C. Tsai, Ph.D., M.S.

Technical Reviewers, in alphabetical order

Martha Sandy, Ph.D., M.P.H.

Meng Sun, Ph.D., M.S.

Rima Woods, Ph.D.

Executive Reviewers

Kimberly Gettmann, Ph.D.

David Edwards, Ph.D.

May 2026 Draft

CONTENTS

LIST OF TABLES

List of Abbreviations

ADH	Alcohol dehydrogenase
AGS	Human Gastric adenocarcinoma
AKR	Aldo-keto reductase
ALDH	Aldehyde dehydrogenase
α-OH-Acr-dGuo	Alpha-hydroxy-1,N2-propano-2´-deoxyguanosine
α-OH-PdG	Alpha-hydroxy-1,N2-propano-2´-deoxyguanosine
BEAS-2B	Human bronchial epithelial cells
BMD	Benchmark Dose
BMDL	95% lower confidence limit for the Benchmark Dose
BMDS	Benchmark Dose Modeling Software
BMR	Benchmark Response
BP	Benzo[a]pyrene
BR_h	Breathing Rate (human)
$BW_{a\ or\ h}$	Body weight (animal or human)
Caco-2	Human intestinal epithelial cells
CARB	California Air Resources Board, The
CEMA	S-carboxyethyl-N-acetylcysteine
CESG	S-(2-carboxyethyl)glutathione
CF	Conversion factor
CFD	Computational fluid dynamic
CHEMA	N-acetyl-S-(2-carboxy-2-hydroxyethyl)-cysteine
CHESG	S-(2-carboxy-2-hydroxyethyl)glutathione
CSF	Cancer Slope Factor
CYP	Cytochrome P450 enzyme
DDR	DNA damage response
°C	Degrees Celsius
DENA	Diethylnitrosamine
DNA	Deoxyribonucleic acid
EH	Epoxide hydrolase
8-OHdG	8-Oxo-2'-deoxyguanosine
FMO	Flavin-containing monooxygenase
fmol/μmole	Femtomole per micromole
γ-H2AX	Phosphorylated form of the histone H2AX
γ-OH-Acr-dGuo	Gamma-hydroxy-1,N2-propano-2´-deoxyguanosine
γ-OH-PdG	Gamma-hydroxy-1,N2-propano-2´-deoxyguanosine
GES-1	Human gastric epithelial cells
GFR	Glomerular filtration rate
GSH	Glutathione
HIF-1α	Hypoxia-inducible factor 1α
HPA	3-hydroxypropanoic acid
HPMA	S-(3-hydroxypropyl)-N-acetylcysteine
HPSG	S-(3-hydroxypropyl)glutathione
HR	Hazard ratio
HUVEC	Human umbilical vein endothelial cells
IARC	International Agency for Research on Cancer, The
IR	Inhalation rate
IUR	Inhalation Unit Risk Factor (from OEHHA)
JBRC	Japan Bioassay Research Center, The
MAP	Mercapturic acid pathway
MDL	Minimum detection limit
mg/kg-d	Milligrams per kilogram of body weight per day
mg/m^3	Milligrams per cubic meter
$μg/m^3$	Micrograms per cubic meter
μmol	Micromole
μmol/L	Micromoles per liter
NA	Not applicable
NaCl	Sodium chloride
NATA	National Air Toxics Assessment
NIH/3T3	Mouse fibroblast cells

List of Abbreviations (continued)

NOKSI	Normal oral keratinocyte spontaneously immortalized cells
NS	Not significant
OEHHA	Office of Environmental Health Hazard Assessment, The
OPSG	S-(3-oxopropyl)-N-acetylcysteine
OR	Odds Ratio
PAH	Polycyclic Aromatic Hydrocarbon
$(mg/kg\text{-}d)^{-1}$	Per milligram per kilogram of body weight per day
$(\mu g/m^3)^{-1}$	Per microgram per cubic meter
$(ppb)^{-1}$	Per part per billion
ppb	Parts per billion
ppm	Parts per million
SMOX	Spermidine Oxidase
SW480 cells	Human colorectal adenocarcinoma cells
TSD	Technical Support Document
TUNEL	Terminal deoxynucleotidyl transferase-mediated dUTP nick end labelling assay
URT	Upper respiratory tract
US EPA	United States Environmental Protection Agency, The
VOC	Volatile Organic Compound

PREFACE

The Office of Environmental Health Hazard Assessment (OEHHA) is legislatively mandated to develop guidelines for conducting health risk assessments under the Air Toxics Hot Spots Program (Health and Safety Code section 44360(b)(2)). In response to this statutory requirement, OEHHA developed a Technical Support Document (TSD) that describes the methodology for deriving inhalation unit risk factors (IURs) and cancer slope factors (CSFs) for carcinogenic Hot Spots air pollutants. The methodology in the TSD explicitly considers possible differential effects on the health of infants, children, and other sensitive subpopulations under the mandate of the Children's Environmental Health Protection Act (Senate Bill 25, Escutia, Chapter 731, Statutes of 1999, Health and Safety Code Sections 39669.5 et seq.), including procedures for evaluating increased susceptibility to carcinogens.

The IUR defines the excess cancer risk associated with continuous inhalation exposure to a given carcinogen at 1 microgram per cubic meter ($\mu g/m^3$) over a lifetime. The CSF estimates excess lifetime cancer risk associated with exposure at 1 milligram per kilogram of body weight per day (mg/kg-d). In the Hot Spots Program, the IUR and CSF are used for calculating cancer risks from chemical exposures above the background levels.

The current document summarizes the carcinogenicity data supporting OEHHA's derivation of a proposed acrolein IUR for public comment under the Air Toxics Hot Spots Program. Acrolein is classified by the International Agency for Research on Cancer (IARC) as probably carcinogenic to humans (Group 2A).

The literature summarized and referenced in the present document covers the relevant publicly available reports and original research reviewed and supported by authoritative bodies for acrolein through April 2026. Individual reports summarized herein were primarily those that would be useful for deriving or supporting an IUR for acrolein, including experimental animal carcinogenicity studies and genetic toxicity studies. Key acrolein studies investigating human exposure, toxicokinetics, and mechanisms of carcinogenicity were also summarized in the present document.

The document is being released for public comment via written submissions and public workshops in Northern and Southern California. Because of the level of scientific information below, those using reading-assistive software should consider enabling the pronunciation of punctuation and symbols and listen for links to footnoted text. OEHHA's website has information about how to engage in the public review process. The comment period closes on June 29, 2026. Public comments will be considered in the revised draft document, which will be reviewed by the Scientific Review Panel on Toxic Air Contaminants.

ACROLEIN

Chemical Abstracts Service Registry Number: 107-02-8

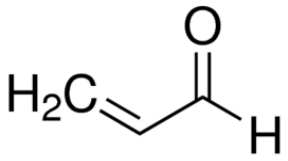

I. PHYSICAL AND CHEMICAL PROPERTIES

(NOAA, 2024; NCBI, 2024; Ghilarducci & Tjeerdema, 1995)

Molecular formula:	C_3H_4O
Molecular weight:	56.06 grams per mole
Conversion factor:	1 part per billion (ppb) = 2.29 micrograms per cubic meter ($\mu g/m^3$)
Synonym:	Acraldehyde; acrylaldehyde; acrylic aldehyde; allyl aldehyde; ethylene aldehyde; propenal; 2-propenal
Description:	Colorless to yellowish liquid with extremely acrid, pungent, and irritating odor
Relative gas density:	1.94 (Air = 1); heavier than air
Specific gravity:	0.8389 at 20 °C
Boiling point:	52.00 to 53.00 °C @ 760.00 mm Hg
Melting point:	–87.8 °C
Vapor pressure:	217.5 mm Hg (29 kPa) at 20 °C
Solubility:	Soluble in ethanol, ether, and acetone; soluble in water (211 g/L at 20 °C)
Odor perception:	0.07 milligrams per cubic meter (mg/m^3); [0.03 parts per million (ppm)]
Odor recognition:	0.48 mg/m^3 (0.21 ppm)

II. HEALTH ASSESSMENT VALUES

Inhalation Unit Risk Factor (IUR):	7.9×10^{-4} per microgram per cubic meter $((\mu g/m^3)^{-1})$; 3.4×10^{-4} per part per billion $((ppb)^{-1})$
Cancer Slope Factor (CSF):	2.8 per milligram per kilogram of body weight per day $((mg/kg\text{-}d)^{-1})$

III. OCCURRENCE AND MAJOR USES

Acrolein is frequently present in ambient air from combustion of fuels, woods, and plastics (OEHHA, 2014; CARB, 1997; Jiang et al., 2022; Burcham, 2017). Acrolein is released in routine emissions from California refineries (OEHHA, 2019) and has been found at elevated levels in neighborhoods located near oil and gas operations (CARB, 2025b), in wildfire smoke (Rice et al., 2023), and in hazardous waste sites (Faroon et al., 2008). It is a major component in tobacco smoke and e-cigarette vapor (Hikisz & Jacenik, 2023b; Cheng et al., 2022). It is also generated during the cooking of food (Hikisz & Jacenik, 2023a). Among the 362 gasoline-related volatile organic compounds (VOCs), acrolein was identified by OEHHA as one of the 29 with known or suspected carcinogenicity or respiratory toxicity; its gasoline-related emissions ranked within the first tertile of all such VOCs in 2012 (0.597 tons/day; OEHHA, 2018a). Acrolein is also a product of the photooxidation of various hydrocarbon pollutants, and an estimated 39% of total acrolein emissions were formed through secondary reactions (OEHHA 2018a).

Tropospheric removal of acrolein is primarily by reactions with hydroxy radicals (Ghilarducci and Tjeerdema, 1995). Atmospheric residence times from 13.5 to 20 hours were measured in the presence of the hydroxyl radical (•OH).

The California Air Resources Board (CARB) established a network of air monitors in urban/suburban regions of California to determine airborne concentrations of toxic substances. Acrolein is one of approximately 80 substances that are, or have been, monitored. Air samples are collected over a 24-hour period every 12 days at 14 sites in California. The most recent year for complete statewide monitoring data for acrolein was 2024, in which the mean concentration was 0.57 $\mu g/m^3$ (0.25 ppb) with site averages ranging from 0.34 to 3.2 $\mu g/m^3$ (0.15 to 1.4 ppb; CARB, 2025a).

Prior to 2024, the most recent year with complete data for statewide monitoring for acrolein was 2019, in which the mean concentration was 1.05 $\mu g/m^3$ (0.46 ppb), with site averages ranging from 0.34 to 9.4 $\mu g/m^3$ (0.15 to 4.1 ppb). From 2020 to 2023, air monitoring for acrolein by CARB was limited, either because acrolein was below the limit of detection of 0.7 $\mu g/m^3$ (0.3 ppb) or because analysis for acrolein was not conducted. For comparison, the concentration of acrolein in indoor settings where people are smoking, such as bars and taverns, ranges from 2.3 to 275 $\mu g/m^3$ (1 to 120 ppb; Faroon et al., 2008; IARC, 1995). The mean concentration of acrolein in downwind communities in the Western US on days impacted by wildfire smoke was 0.65 $\mu g/m^3$ (0.28 ppb), with a mean absolute difference for smoke impacted days compared to non-smoke days of 0.16 $\mu g/m^3$ (0.070 ppb; Rice et al., 2023).

Depending on canister preparation for air sampling, the concentration of acrolein may increase in the canisters prior to analysis (US EPA, 2010). In addition, the accuracy of acrolein gas standards used to calibrate GC/MS equipment can vary considerably between laboratories. Cahill (2014) measured concentrations of acrolein in remote, rural, and urban areas in California between September and October 2013 using a mobile battery powered sampling mist chamber system that was specifically designed for acrolein analysis. This method avoids the quality control concerns of methods used in other laboratories. In remote and coastal areas, the acrolein concentrations ranged from below the minimum detection limit (MDL) of 0.041 $\mu g/m^3$ (0.018 ppb) to a maximum of 0.16 $\mu g/m^3$ (0.070 ppb) (n = 40). Most of these samples were at or below the MDL. In the Los Angeles Basin, the concentration ranged from 0.23 to 0.41 $\mu g/m^3$ (0.10 to 0.18 ppb) with a median of 0.32 $\mu g/m^3$ (0.14 ppb) (n = 8). The acrolein concentration range measured by CARB in Los Angeles was <MDL to 3.7 $\mu g/m^3$ (1.6 ppb) in 2013.[1]

While acrolein's presence in the air is caused by many sources, it is also directly used as an aquatic herbicide to control underwater plants, algae, and slime growth in both agricultural and non-agricultural (i.e., urban, industrial and rights-of-way) settings in California (DPR, 2021; DPR, 2022; CARB, 1997). Other registered pesticide uses are as a bactericide, antimicrobial agent, for vertebrate control (i.e. fumigant for burrowing rodents) and as a disinfectant (DPR, 2024; Burcham, 2017). In California, there are currently two actively registered pesticidal products that contain acrolein. Industrial uses include addition to recirculating process water systems to control mollusks, the control of slime formation in paper manufacturing, and as a biocide and hydrogen sulfide scavenger in upstream oil and natural gas production processes (IARC, 2021; Garcia-Gonzales et al., 2019).

IV. CARCINOGENICITY

Following release of carcinogenicity bioassays in rats and mice by the Japan Bioassay Research Center (JBRC, 2016a,b; Matsumoto et al., 2021), IARC (2021) conducted a review of all the available carcinogenicity studies in animals and concluded that there is sufficient evidence that acrolein is carcinogenic in experimental animals. IARC categorized acrolein as probably carcinogenic to humans (a Group 2A carcinogen). The Group 2A evaluation for acrolein is based on sufficient evidence of cancer in experimental animals (increased nasal tumor formation in both rodent species exposed to acrolein via inhalation) and strong

[1] Analytical methods used by CARB in 2013 differed from that used by CARB in 2024. Thus, the acrolein concentrations from these sources are not strictly comparable.

mechanistic evidence that “acrolein exhibits multiple key characteristics of carcinogens, primarily from studies with human primary cells and studies in experimental systems, supported by studies in humans for DNA adducts.” (IARC, 2021).

Few human epidemiological studies on the carcinogenicity of acrolein were found in the literature by IARC (2021). At that time, IARC concluded there was inadequate evidence in humans regarding the carcinogenicity of acrolein, noting that “the studies were either of poor quality regarding design or exposure assessment, or they were of a mechanistic nature”.

Subsequent to IARC’s assessment, OEHHA performed a literature search focused on key studies in Human Cancer, Experimental Animal Cancer, and Genotoxicity. Searches were executed in PubMed, Embase, and Scopus. Searches were performed in July 2024 and September 2025.

Rodent Carcinogenicity Studies

Two reports (Feron & Kruysse, 1977; Matsumoto et al., 2021[2]) have been published that characterized the carcinogenicity of acrolein by the inhalation route. Experimental animals studied include rats, mice, and hamsters.

Matsumoto et al. (2021); JBRC (2016a,b)

Tumor incidence in F344/DuCrlCrlj (SPF) rats

In two-year carcinogenicity and chronic toxicity inhalation bioassays, male and female F344/DuCrlCrlj (SPF) rats (n = 50/sex/exposure group) were exposed to acrolein at concentrations of 0, 0.2, 1.1, or 4.6 mg/m^3 (0, 0.1, 0.5, or 2 ppm) 6 hours/day, 5 days/week for 104 weeks. Survival rates of the male rat groups were unaffected by acrolein exposure. In females, the survival rate in the 4.6 mg/m^3 group decreased below that of the control group late in the study (after week 90). The overall survival rates in females at the end of the two-year exposures were 86, 84, 82, and 68% in the 0, 0.2, 1.1, or 4.6 mg/m^3 groups, respectively. Mean terminal body weight (BW) of male rats was reduced in the 0.2 ($p < 0.05$) and 4.6 mg/m^3

[2] Matsumoto et al. (2021) is based on the two-year inhalation studies conducted by the Japan Bioassay Research Center (JBRC) in female B6D2F$_1$/Crlj mice and female F344/DuCrlCrlj rats (JBRC, 2016 a, b).

($p < 0.01$) exposure groups. The mean terminal BW of females was reduced in the 4.6 mg/m^3 group ($p < 0.05$).

For tumor incidence in Table 1, statistical pairwise comparisons with controls were performed by OEHHA using Fisher's exact test. Statistical trend analysis for tumor incidence was performed by OEHHA using the exact conditional Cochran-Armitage test for linear trend (i.e., exact trend test) as recommended by US EPA (2005) for carcinogen risk assessment. In addition to the Cochran-Armitage test, Matsumoto et. al. also analyzed the tumor incidence data using the Peto's trend test[3] (JBRC, 2016a).

The statistically significant and biologically noteworthy tumor incidences in male and female rats are shown in Table 1. In the 4.6 mg/m^3 groups, squamous cell carcinoma of the nasal cavity was observed in one male rat and two female rats. Although the incidence of this tumor was not statistically significantly increased in either sex, it did exceed the JBRC laboratory historical control incidence in both males (0/599) and females (0/600). The authors attributed these nasal tumors to be related to acrolein exposure. Exposure-related non-cancer lesions of the nasal cavity included a statistically significant increase in squamous cell metaplasia in respiratory epithelium and hyperplasia in transitional epithelium ($p < 0.01$) of males and females in the 4.6 mg/m^3 groups. The authors believed these to be pre-neoplastic lesions that can give rise to squamous cell carcinoma.

In addition to squamous cell carcinoma, rhabdomyoma of the nasal cavity was observed in four female rats in the 4.6 mg/m^3 group. Although the increased incidence of this tumor did not reach statistical significance by pairwise comparison with the control group ($p = 0.059$), the incidence did exceed the JBRC laboratory historical control rate (0/600). This finding resulted in a significant positive trend in the incidence of rhabdomyoma ($p < 0.01$, exact trend test). The authors considered these tumors to be exposure-related. The presence of striated muscle proliferation in the same region of the nasal cavity (dorsal area) that rhabdomyomas were found were

[3] Peto's trend test was developed to account for differential intercurrent mortality between groups in a long-term carcinogenicity study (Peto et al., 1980). In Peto's test, tumors are classified by study pathologists' evaluation as incidental (tumors found at death but were considered not to be cause of death) or fatal (tumors caused death). JBRC (2016a) conducted three different calculations based on the context of tumor observation: prevalence method (for incidental tumors), standard method (for fatal tumors), and the combined method (when the same type of tumor appeared to be incidental in some animals and fatal in others).

192 significantly increased in 4.6 mg/m^3 males and females and thought to be pre-
193 neoplastic lesions for this tumor type.

194 JBRC (2016a) reported that the combined incidence of nasal cavity squamous cell
195 carcinoma and rhabdomyoma in female rats in the 4.6 mg/m^3 group was 6 out of 50,
196 which was statistically significant by pairwise comparison to controls (Table 1). While
197 IARC's (2021) Working Group noted that squamous cell carcinoma and
198 rhabdomyoma have different histotypes, they considered the combined incidence of
199 these two tumors to be rare and exposure-related.

200 Pair-wise comparison with the control group did not result in a significantly increased
201 incidence in any of the exposed groups for pituitary adenomas and
202 adenocarcinomas, either separately or combined. In female rats, the trends for
203 pituitary adenomas alone and for combined pituitary adenomas and
204 adenocarcinomas were statistically significant ($p < 0.05$) by the Peto's trend test
205 (Matsumoto et al., 2021; JBRC, 2016a) but not the Cochran-Armitage trend test
206 (Table 1). The incidence of pituitary adenomas in all exposure groups was within the
207 historical range in the JBRC data: 165/599 (27.5%, range: 22–42%).

208 This was the only occurrence in which statistical significance using the Peto's trend
209 test (standard method) and Cochran-Armitage trend tests diverged for a specific
210 tumor at $p < 0.05$. The JBRC uses both the Cochran-Armitage and Peto's trend tests
211 in their assessment of carcinogenicity in animal models. IARC (2021) concluded that
212 the pituitary gland tumors observed in the female rat study may not be related to
213 acrolein exposure due to the high background incidence of pituitary gland adenoma
214 in ageing rats, the absence of an increased incidence of this tumor in male rats, and
215 the lack of a significant increase in pituitary gland adenocarcinoma.

Table 1. Incidence of primary tumors in male and female rats exposed by inhalation to acrolein for two years (JBRC, 2016a; Matsumoto et al., 2021)[a].

Sex	Tumor Type	Cancer Incidence by Acrolein Exposure Concentration				Trend test *p*-value [b]
		0 mg/m^3, 0 ppm	0.2 mg/m^3, 0.1 ppm	1.1 mg/m^3, 0.5 ppm	4.6 mg/m^3, 2 ppm	
Male	Nasal cavity: Squamous cell carcinoma	0/50	0/50	0/50	1/50	0.25
Female	Nasal cavity: Squamous cell carcinoma	0/50	0/50	0/50	2/50	0.062
	Nasal cavity: Rhabdomyoma	0/50	0/50	0/50	4/50[c]	0.0036
	Nasal cavity: Squamous cell carcinoma and rhabdomyoma (combined)	0/50	0/50	0/50	6/50*	0.00019
	Pituitary gland: Adenoma	14/50	15/50	20/50	17/50	0.32[d]
	Pituitary gland: Adenocarcinoma	0/50	2/50	1/50	0/50	0.74
	Pituitary gland: Adenoma and adenocarcinoma (combined)	14/50	17/50	21/50	17/50	0.40[e]

Abbreviations: JBRC – Japan Bioassay Research Center; mg/m^3 – milligrams per cubic meter; ppm – parts per million.

(a) Statistical pairwise comparisons with controls for cancer incidence were performed by OEHHA using Fisher's exact test; * *p*-value < 0.05, ** *p*-value < 0.01

(b) The exact trend test was performed by OEHHA

(c) *p*-value = 0.059 by Fisher's exact test

(d) Peto's trend test: *p*-value by standard method = 0.0115, *p*-value by prevalence test = 0.5619, *p*-value by combined analysis = 0.1619 (JBRC, 2016a)

(e) Peto's trend test: *p*-value by standard method = 0.0215, *p*-value by prevalence test = 0.6199, *p*-value by combined analysis = 0.2243 (JBRC, 2016a)

Shu et al. (2017) stated a limitation of Peto's test: "Although the exact Peto's test overcomes C-A test by adjusting the mortality among treatment groups, it highly relies on the tumor context classification from pathologists, which may be subjective and may render the information too inaccurate to allow valid analysis". Peto et al. (1980) noted that pituitary tumors can be both observed in the incidental context and

the fatal context, so there can be instances when the experimenter cannot be certain if the pituitary tumor was the underlying cause of death.

In another analysis of trend tests, Kodell et al. (2012) summarized the recommendations of the Society of Toxicologic Pathology (STP Working Group, 2002) by stating that the Peto's test should be performed whenever the study pathologist and peer-review pathologist can consistently classify neoplasms as fatal or incidental. If fatal and incidental classifications are not applied, then the Poly-3 or another alternative to the Peto's test should be employed.

Tumor incidence in B6D2F1/Crlj (SPF) mice

Matsumoto et al. (2021) also conducted acrolein carcinogenicity and chronic toxicity inhalation bioassays in male and female B6D2F1/Crlj (SPF) mice (n = 50/sex/exposure group). The animals were exposed to 0, 0.2, 0.9, or 3.7 mg/m^3 (0, 0.1, 0.4, or 1.6 ppm) acrolein for 6 hours/day, 5 days/week. Due to decreased survival rates in all exposure groups, the study was terminated in the 93rd week for males and the 99th week for females. No differences in terminal survival were observed between the control and acrolein-exposed groups. Decreased survival was due to nephrosclerosis of the kidney and/or deposition of amyloid in various organs and was not considered exposure-related. Body weights of males in the 3.7 mg/m^3 group were reduced throughout the study, and up to the 82nd week of exposure in females in the 3.7 mg/m^3 group.

A statistically significantly increased incidence of adenomas of the nasal cavity ($p < 0.01$) was observed in 3.7 mg/m^3 females (Table 2). A significant positive trend for this tumor was also observed ($p < 0.01$). Only one 3.7 mg/m^3 male was found to have a nasal cavity adenoma. In laboratory historical controls (JBRC, 2016b), no nasal cavity adenomas occurred in female mice (0/500), and one occurred in male mice (1/500). The authors concluded that the adenomas in 3.7 mg/m^3 females were exposure-related but could not conclude this for the 3.7 mg/m^3 males. IARC noted that the 2% incidence (1/50) of nasal cavity adenoma in males was in the upper bound of the historical control range: (0.2%, range: 0–2%).

Significant increases in non-neoplastic lesions in the nasal cavity were observed primarily in 3.7 mg/m^3 male and female mice. In particular, a significant increase in inflammation and hyperplasia occurred in the respiratory epithelium of 3.7 mg/m^3 males and 0.9 and 3.7 mg/m^3 females. These lesions were considered by the authors to be precursors to nasal tumors.

In neoplastic findings outside the upper respiratory tract, the incidence of histiocytic sarcoma of the uterus was significantly increased ($p = 0.039$) in 0.9 mg/m^3 female

mice compared to the control group, but the incidence of this tumor was not significantly increased in the highest exposure (3.7 mg/m^3) group (Table 2). Consequently, a statistically significant positive trend was not attained (p = 0.87) for this tumor type. The JBRC laboratory historical control range for histiocytic sarcoma was 114/500 (22.8%, range: 18–34%). The percent incidence for this neoplasm was below the lower end of the historical range in the control and 3.7 mg/m^3 groups (the incidence in 0, 0.2, 0.9, or 3.7 mg/m^3 female mice was 12, 26, 28, and 12%, respectively). IARC (2021) stated that although a clear dose-response trend was not observed, the increase in histiocytic sarcoma in female mice may have been related to acrolein exposure.

Histiocytic sarcomas in female mice were also found in the liver (two in the 0.2 mg/m^3 group and three in the 3.7 mg/m^3 group), subcutis (one in the control group and one in the 0.9 mg/m^3 group), spleen (one in the 3.7 mg/m^3 group), vagina (one in the 0.2 mg/m^3 group), and Harderian gland (one in the 3.7 mg/m^3 group). Brix et al. (2010) notes that most neoplasms of the same histomorphogenic type can be combined even if they occur in different anatomic sites (i.e., histiocytic sarcoma in different organs). It was not clear in the reporting of the study if multiple histiocytic sarcomas in different organs were present in some of the same mice. Therefore, tumor incidence can only be determined for these tumors by organ site.

Other non-respiratory tract neoplasm findings included a significant positive trend (p = 0.020) for malignant lymphoma of the lymph node. The incidence of lymphoma was not significantly increased (i.e., $p \leq 0.05$) in each exposure group compared to control (OEHHA calculated a p = 0.19 for the highest exposure group compared to control). The JBRC laboratory historical control range for malignant lymphoma was 169/500 (33.8%, range: 28–46%). IARC's Working Group (Marques et al., 2021; IARC, 2021) concluded that malignant lymphoma in female B6D2F1/Crlj mice was a treatment-related finding.

Malignant lymphoma of the spleen was also observed in one female mouse in the high-dose group (3.7 mg/m^3), which Brix et al. (2010) suggests can be combined with malignant lymphomas at other anatomic sites. However, it was not specified in the cancer bioassay if this lymphoma occurred in a mouse that did not also have malignant lymphoma of the lymph node.

Table 2. Incidence of primary tumors in male and female mice exposed by inhalation to acrolein (JBRC, 2016b; Matsumoto et al., 2021)[a].

Sex	Tumor Type	Cancer Incidence by Acrolein Exposure Concentration				Trend test *p*-value [b]
		0 mg/m^3, 0 ppm	0.2 mg/m^3, 0.1 ppm	0.9 mg/m^3, 0.4 ppm	3.7 mg/m^3, 1.6 ppm	
Male	Nasal cavity: Adenoma	0/50	0/50	0/50	1/50	0.25
Female	Nasal cavity: Adenoma	0/50	0/50	0/50	16/50**	< 0.0001
	Uterus: Histiocytic sarcoma	6/50	13/50	14/50*	6/50	0.87
	Lymph node: Malignant lymphoma	12/50	8/50	6/50	17/50	0.020

Abbreviations: JBRC – Japan Bioassay Research Center; mg/m^3 – milligrams per cubic meter; ppm – parts per million.

(a) Statistical pairwise comparisons with controls were performed by OEHHA using Fisher's exact test; * *p*-value < 0.05, ** *p*-value < 0.01.

(b) The exact trend test was performed by OEHHA.

Feron and Kruysse (1977)

In this study, effects of acrolein exposure alone or in the presence of other carcinogens (benzo[a]pyrene [BP] and diethylnitrosamine [DENA]) were investigated using male and female Syrian Golden hamsters.

The treatments groups are shown in Table 3. Animals from each treatment group were divided into two exposure chambers. One chamber was a control chamber, where the animals were exposed to filtered and conditioned air. The other chamber was the test chamber, where the animals were exposed to an average concentration of 9.2 mg/m^3 (4 ppm) of acrolein for 7 hours/day, 5 days/week. Exposure in all groups continued for 52 weeks, followed by a 29-week post-exposure period in clean air.

A complete autopsy was performed on all animals. Histological examination of the respiratory tract was conducted only on grossly visible tumors or lesions suspected of being tumors. In addition, three males and females from the groups not treated with BP or DENA were sacrificed and examined at the end of 52 weeks of exposure.

Table 3. Study design of Feron & Kruysse (1977).

Treatment (other than inhalation)	Exposure Route and Frequency	Number of Animals per Sex	Exposure in Inhalation Chamber
None	Not applicable	18	Filtered air
None	Not applicable	18	Acrolein
0.9% NaCl	Intratracheal installation once a week	18	Filtered air
0.9% NaCl	Intratracheal installation once a week	18	Acrolein
0.175% BP in 0.9% NaCl	Intratracheal installation once a week	30	Filtered air
0.175% BP in 0.9% NaCl	Intratracheal installation once a week	30	Acrolein
0.35% BP in 0.9% NaCl	Intratracheal instillation	30	Filtered air
0.35% BP in 0.9% NaCl	Intratracheal instillation	30	Acrolein
0.0675% DENA in 0.9% NaCl	Subcutaneous injection once every three weeks	30	Filtered air
0.0675% DENA in 0.9% NaCl	Subcutaneous injection once every three weeks	30	Acrolein

Abbreviations: BP – Benzo[a]pyrene; DENA – Diethylnitrosamine; NaCl – Sodium Chloride

Males and females exposed to acrolein-only showed a roughly 10% loss in BW by week 52, but differences in BW gradually decreased up to week 81 during the post-exposure period. No treatment-related reduction in survival occurred during the study, although female hamster survival overall was low by week 81. Survival rates were 77%, 77%, 47%, and 57% for control males, acrolein-only exposed males, control females and acrolein-only exposed females, respectively.

Lesions in the acrolein-only exposed animals were observed in the anterior half of the nasal cavity and consisted of inflammation and slight-to-moderate metaplasia. At the end of 81 weeks, 20% of the animals still showed nasal cavity lesions that consisted mainly of thickened submucosa and exudation in the lumen. A small tracheal papilloma was found in one acrolein-exposed female that was not considered by the

authors to be related to exposure. No other respiratory tract tumors were found in control or acrolein-only male and female hamsters.

A slight but non-significant increase in respiratory tract tumor incidence occurred in females exposed to both acrolein and BP compared to females administered BP only (11%, 28%, 29% and 50% tumor incidence for low-dose BP-only, low-dose BP plus acrolein, high-dose BP-only, and high-dose BP plus acrolein, respectively). A significant shortening of the latency period for appearance of respiratory tract tumors was observed in BP-exposed females that were also exposed to acrolein. No increase in respiratory tumors was observed in acrolein-exposed males also administered BP. Exposure to DENA did not result in significant differences in incidence, site, or type of respiratory tract tumors between hamsters exposed to air and those exposed to acrolein vapor.

Limitations of the hamster carcinogenicity bioassays noted by IARC (2021) included the small number of animals per group, the short duration of the exposure (i.e., one-year), the low survival rate in females, the use of a single acrolein dose, and the reporting of pathological data mostly limited to the respiratory tract tumors.

Epidemiological Studies

Two occupational studies and four population-based studies were reviewed by IARC (2021). OEHHA's literature search identified an additional six population-based studies published subsequent to IARC's review.

Only two published occupational studies included acrolein in their assessment for carcinogenic risk that resulted primarily from inhalation exposure. However, air monitoring data was not collected for acrolein, and there was inadequate information for the carcinogenic effects of acrolein due primarily to concurrent airborne exposure to multiple chemicals, especially to other carcinogens. Ten population-based studies were identified that examined associations between acrolein or its metabolites and cancer. Among these population-based studies, two of them are informative for the carcinogenicity evaluation of acrolein.

Occupational Studies

In a small occupational study, Bittersohl (1975) reported on the number of neoplasms among workers in the hydrogenation unit of a German aldehyde factory. Ambient concentrations of some aldol and aliphatic aldehydes were measured, including acetaldehyde (1–7 mg/m^3), butyraldehyde (5–70 mg/m^3), crotonaldehyde (1–7 mg/m^3), n-butanol (2–6 mg/m^3) and ethylhexanol (about 15 mg/m^3). No exposure assessment was conducted for acrolein, and the authors assumed that

employees in the hydrogenation unit were exposed to acrolein as a trace byproduct potentially formed during the dimerization of acetaldehyde to produce acetaldol. Bittersohl (1975) reviewed the medical records of 220 plant workers, 150 of whom were followed for over 20 years from the start of the study through its conclusion. Malignant neoplasms were found in nine males with a sufficient latency period (mean latency for the nine workers with neoplasms was 26 ± 4 years). These consisted of two squamous cell carcinomas of the oral cavity, five squamous cell carcinomas of the bronchial tree, one adenocarcinoma of the stomach, and one adenocarcinoma of the caecum. The authors observed that the number of bronchial neoplasms were above the average for the then German Democratic Republic and findings in its chemical industry. The authors used cancer counts instead of rate as a report of effect size, and they compared the number of cases in the factory with the proportion of cancer cases in the general population instead of cancer rates. The study was limited by the absence of data on acrolein concentrations and exposures in the workplace, and the absence of an appropriate effect estimate and comparison group. Overall, this study was considered uninformative. Ott et al. (1989 a, b) conducted a nested case-control study of 129 male cases with multiple myeloma, non-Hodgkin's lymphoma, and leukemia; and 645 controls selected from 774 employees at two large West Virginia chemical manufacturing facilities and a research and development center. Cases were identified according to death certificate diagnosis which might have resulted in misclassification bias. Individual chemical exposures were assessed by linking each employee’s work assignments to historical departmental use of specific substances. Such retrospective and indirect exposure assessment may have resulted in an information bias that could be either differential or nondifferential between cases and controls. Only 25 men (12.5%) were ever exposed to acrolein, and only three were exposed for more than five years. The employees exposed to acrolein were also exposed to numerous other chemicals. Correlation analysis showed that acrolein shared a high correlation coefficient with epichlorohydrin (a known carcinogen). Positive associations were found between acrolein exposure and non-Hodgkin lymphoma (odds ratio (OR) = 2.6, n = 2), multiple myeloma (OR = 1.7, n = 1), and leukemia (OR = 2.6, n = 3). However, it was noted that the 95% confidence intervals—which were not reported in the paper—were wide and included 1, indicating a lack of statistical significance. Additionally, the observed associations were based on very small sample sizes, limiting the reliability of the findings. Numerous positive associations were also reported between lymphatic or hematopoietic malignancies and other known carcinogens including benzene, formaldehyde, vinyl chloride, and ethylene oxide. Given several limitations, including potential bias and confounding, there is considerable uncertainty in the reported associations between acrolein exposure and these lymphohematopoietic cancers.

IARC (2021) noted that the main limitations of these two occupational studies (Bittersohl et al.,1975; Ott et al., 1989 a, b) included a lack of quantitative exposure assessment and simultaneous exposure to multiple chemical substances.

Population-based Studies

OEHHA's literature search identified four population-based studies that were summarized by IARC (2021) and six studies published since the IARC review.

IARC (2021) found the four population-based studies included in its review to be uninformative. Specifically, the case–control study on urothelial cancer in patients with chronic kidney disease (Hong et al., 2020) was considered uninformative due to small numbers, poor external exposure assessment, and flaws in design. One case–control study detected higher levels of acrolein–DNA adducts in buccal swabs of patients with oral cancer compared with healthy controls but did not find an association between adduct levels and external exposures, including tobacco smoking or betel chewing (Tsou et al., 2019). Two nested case–control studies (Yuan et al., 2012, 2014) in a population-based cohort studied several biomarkers (including metabolites of acrolein) in relation to lung cancer among current smokers and non-smokers respectively, without demonstrating a direct etiological involvement of acrolein.

The population-based studies identified after IARC (2021) included one prospective cohort study (Feng et al., 2024), three case control studies (Rodriguez et al., 2024, Peterson et al., 2025 and Etemadi et al., 2024), and one retrospective cohort study (Heck et al., 2024). The first four studies (Feng et al., 2024; Rodriguez et al., 2024; Peterson et al., 2025, and Etemadi et al., 2024;) examined the association between levels of acrolein metabolites and cancer risk or mortality, while the fifth study (Heck et al., 2024) examined residential exposure to acrolein in ambient air and breast cancer risk. Among these studies, Etemadi et al. (2024) and Heck et al. (2024) provide some information relevant to evaluating the possible association between exposure to acrolein and cancer. The remaining studies are uninformative due to several limitations such as incomplete consideration of exposure sources, small sample size, use of a single urine sample, residual confounding, and reverse causation. Each of the population-based studies are discussed in more detail below.

Yuan et al. (2012) included 343 cases and 392 controls (all smokers) from the Shanghai cohort followed from 1986 through 2006. There was a 2-fold higher risk of lung cancer (OR = 2.0; 95% Confidence Interval [CI] 1.25–3.20; *p* trend = 0.004) between the highest quartile of HPMA levels compared to the lowest quartile when adjusted for intensity and duration of smoking at baseline. However, the effect disappeared upon further adjustment for other polycyclic aromatic hydrocarbon

(PAH) metabolites, tobacco specific nitrosamines, and/or cotinine. In another study using the same cohort data, Yuan et al. (2014) included 82 cases and 83 controls (all non-smokers, although exposure to secondhand smoke was not examined) with follow up through 2008. No association was observed between urinary HPMA levels (highest vs. lowest quartile) and lung cancer risk after adjusting for potential confounders, including cotinine. IARC (2021) noted the limitations of these two studies. For example, IARC considered Yuan et al. (2012) not informative for the carcinogenicity of acrolein since effects disappeared with adjustment for other biomarkers associated with smoking. Yuan et al. (2014) lacked external exposure assessment, and urinary cotinine may not fully represent long-term secondhand smoking exposure.

A case-control study was performed to investigate the role of acrolein in the development of urothelial carcinoma in cancer patients with chronic kidney disease (Hong et al., 2020). Participants were recruited in Taiwan between 2016 and 2019 and included 62 urothelial carcinoma cases with chronic kidney disease, as well as 43 healthy controls with normal kidney function, defined by glomerular filtration rate (GFR) of 143.2 ± 26.9 ml/min/1.73 m². Chronic kidney disease stage classification was also determined in urothelial carcinoma cases by estimating GFR. Acrolein-DNA adduct levels in urothelial carcinoma cells were 1.2-fold higher than in normal urothelial cells from controls ($p < 0.005$) and adduct levels were significantly higher in cancer cases with late-stage chronic kidney disease versus early-stage disease. Acrolein-conjugated protein levels in the plasma of cases were 2-fold higher than in controls ($p < 0.001$). Similar results were observed for both acrolein-DNA adducts and acrolein-conjugated protein levels when comparing only non-smoker cases and controls. Urinary HPMA levels were significantly lower in cases than in controls. IARC (2021) noted a number of limitations of this study, including small sample size and short follow up time. Other limitations of this study are the possibility for reverse causation, and residual confounding.

Tsou et al. (2019) performed a case-control study in Taiwan with 97 cases with oral cancer and 230 healthy subjects, recruited in 2016–2018. Information on cigarette smoking and chewed betel quid (a mixture of areca nut, slaked lime, and betel leaf) was collected from participants. In participants that smoked or chewed betel quid, acrolein-DNA adducts were 1.4-fold higher in the oral cavity of cases compared to controls ($p < 0.001$). In participants that both smoked and chewed betel quid, cases had 1.3-fold higher levels of acrolein-DNA adducts compared to controls ($p < 0.05$). Within the oral cancer cases, acrolein-DNA adducts were 1.8-fold higher in tumor tissues compared to normal buccal cells ($p < 0.01$). Within the control group, differences in smoking or betel quid use did not influence the levels of acrolein-DNA adducts. HPMA levels in urine were significantly lower in cases, compared to controls

with comparable smoking or betel quid use ($p < 0.001$). Other sources of acrolein exposure were not identified in this study, and IARC (2021) noted that causal inference is difficult since samples from cases were taken after oral cancer diagnosis.

Studies published since IARC (2021)

A nested case control study was conducted, drawing participants from within an ongoing prospective cohort study in Golestan, Iran. This nested case control study examined associations between urinary metabolites of pollutants and the risk of esophageal squamous cell carcinoma (Etemadi et al., 2024). Thirty-three urinary metabolites of PAHs, VOCs, and tobacco-specific nitrosamines were measured in participants in this region, which has one of the highest rates of esophageal cancer in the world. Among the several associations observed in this nested case control study, two acrolein metabolites (HPMA and S-carboxyethyl-N-acetylcysteine [CEMA]) were associated with esophageal squamous cell carcinoma in individuals who did not use tobacco (148 cases and 163 controls). After adjusting for potential confounders (mentioned above), the OR for the 90th percentile exposure compared to the 10th percentile was 2.3 (95% CI: 1.1–4.6) for CEMA and 1.8 (95% CI: 1.0–3.5) for HPMA, among non-tobacco users.

This study had limited statistical power to detect associations between acrolein metabolites and cancer in tobacco users due to the small number of cases who used tobacco (n = 57). However, it also had several notable strengths. Participants completed a comprehensive questionnaire upon enrollment and provided information about tobacco use, opiate use, and household fuel use for heating and cooking (natural gas, kerosene, and biomass). To conduct separate analyses on smokers and non-smokers, the researchers matched cases and controls based on tobacco use (cigarettes, waterpipe, and nass, i.e., a form of oral smokeless tobacco commonly consumed in South Asia) and period of use (never, former, current). The researchers considered various potential confounders including dietary factors, heating and/or cooking fuel type, ethnicity, education, wealth score, BMI, tea temperature, tooth loss, urinary cotinine, and opium use (shown to be strongly associated with cancer in the same study population). Urine samples were collected at baseline, more than 10 years prior to esophageal cancer diagnosis, reducing the likelihood of reverse causation. Urinary biomarkers provided a direct measure of exposure from all potential sources, and any measurement error likely biased the results toward the null, rather than creating false associations.

In an earlier study, the same authors compared concentrations from a second urine sample—collected five years after baseline—with the original measurements, to address concerns about the short half-lives of these urinary biomarkers. They

observed moderate to good correlations, suggesting that these biomarkers may capture longer-term exposure patterns (Etemadi et al., 2019).

Feng et al. (2024) conducted a population-based prospective cohort study in US adults examining the relationship between 15 urinary VOC metabolites, including acrolein metabolites HPMA and CEMA, with all-cause and cause-specific (including cancer) mortality. Data from 8,799 participants in the National Health and Nutrition Examination Survey (NHANES) were analyzed across five survey cycles: 2005–2006, 2011–2012, 2013–2014, 2015–2016, and 2017–2018. The Cox proportional hazards models were adjusted for potential confounders including sex, age, BMI, drinking status, smoking status, educational levels, marital status, and race/ethnicity. Both adjusted and unadjusted models showed that HPMA and CEMA were significantly associated with increased hazard ratios for all-cause mortality and cancer mortality (i.e., mortality from any type of cancer). Other individual VOC metabolites positively associated with cancer mortality included acrylonitrile, 1,3-butadiene, crotonaldehyde, ethyl benzene, N,N-dimethylformamide, and styrene.

This study had several limitations related to exposure assessment, outcome ascertainment, and the potential for reverse causation. The authors did not specify whether urinary acrolein metabolites were measured across all five NHANES cycles, which is important because not all biomarkers are consistently collected in every cycle. In terms of outcome ascertainment, the authors did not evaluate site-specific cancer mortality but instead assessed mortality from all cancer types combined. Additionally, the lack of temporal clarity between exposure and outcome raises concerns about potential reverse causation.

A nested case cohort study evaluated the association between two urinary metabolites of acrolein (i.e., CEMA and HPMA) and lung cancer (Nalini et al. 2026). The study was nested within the Sister Study, which enrolled participants in the US (including Puerto Rico) between 2003 and 2009. The analysis included 356 incident cases of lung cancer (diagnosed by September 2017) and 433 non-cases.

The adjusted Cox proportional hazard analyses showed a significant positive association between both acrolein biomarkers and lung cancer among the study's "current smokers group" (i.e., current smokers at enrollment), with an HR of 1.74 (95% CI: 1.11–2.72) for CEMA and an HR of 2.07 (95% CI: 1.49–2.88) for HPMA. Positive associations with several other biomarkers of tobacco smoke constituents were also observed in current-smokers, including for naphthalene, phenanthrene, pyrene, fluorene, o-xylene, m-and p-xylene, acrylamide, acrylonitrile, 1,2-dibromoethane, vinyl chloride, ethylene oxide/and acrylonitrile, styrene/ethylbenzene, dimethylformamide, methylisocyanate, 1,3 butadiene, crotonaldehyde, isoprene and

several tobacco specific nitrosamines. After adjusting the analyses for smoking frequency and duration, the positive associations remained significant for HPMA with an HR of 1.59 (95% CI: 1.04–2.24), but not for CEMA with an HR of 1.48 (95% CI: 0.89–2.48). No positive associations between acrolein metabolites and lung cancer were observed after adjusting for these factors and cotinine and hydroxy cotinine (indicators of recent nicotine exposure), with an HR of 1.2 (95% CI: 0.69–2.08) for CEMA and 1.38 (95% CI: 0.89–2.13) for HPMA.

No positive associations were observed between acrolein metabolites and incident lung cancer in the study's "non-current smoking" group (i.e., nonsmokers at enrollment), with an HR of 0.98 (95% CI: 0.71–1.34) for CEMA and 0.96 (95% CI: 0.74–1.26) for HPMA. The null findings for this stratified analysis may be influenced by grouping former smokers together with the never smokers.

The study had several strengths including time to event analysis, adjustment for various potential confounders, and cohort study design. This study's limitations include one-time measurement of exposure (urine sample), smoking classification based on status at time of enrollment, short follow up for a disease (lung cancer) often associated with a longer latency period of 30 years or more, lack of data on lung cancer histological subtypes, and limited generalizability.

A small case control study was performed in 2022–2023 to investigate the correlation of urinary levels of fungal and environmental toxicants and pancreatic ductal adenocarcinoma in Florida (Rodriguez et al., 2024). Study participants were all Caucasian and included 20 pancreatic ductal adenocarcinoma cases and 20 healthy controls. For cases, a single urine sample was provided within one month of pancreatic ductal adenocarcinoma diagnosis. Subjects with pancreatic ductal adenocarcinoma had significantly higher urinary concentration of HPMA ($p < 0.001$) compared to controls. Similar associations were found for three fungal toxins (ochratoxins, citrinin, and gliotoxins), nine other environmental toxicants (methyl tert-butyl ether, xylene, styrene, acrylonitrile, perchlorate, diphenyl phosphate, bromopropane, organophosphates, and diethylphosphate), and one biomarker of mitochondrial dysfunction (tiglylglycine). Limitations of this study include the use of mean difference comparison instead of ratio (relative) measurement, and small sample size. While urinary levels of these chemicals can be used as a screening marker for pancreatic ductal adenocarcinoma, this study is not informative for carcinogenicity of acrolein.

Another small case-control study was conducted to determine the correlation of urinary acrolein metabolite levels with diagnosis of urothelial cell carcinoma (Peterson et al., 2025). Study participants were recruited from the Urology Clinic of

University of Wisconsin-Madison and included 25 newly diagnosed urothelial carcinoma cases and 25 controls with benign urologic disease. All participants were self-reported current non-smokers. HPMA was detected in the urine of all 50 participants and was not significantly different between cases and controls (p = 0.44). Limitations of this study included using samples at a single time point, and control (comparison) group recruitment from the hospital.

In a multiethnic cohort study, the relationship between residential ambient air exposure to eight traffic-related air toxics, including acrolein, and breast cancer risk was examined in 48,665 California female participants followed from 2003 through 2013 (Heck et al., 2024). All participants lived in the Los Angeles air basin. Including 5-year lagging, all traffic-related pollutants consistently exhibited positive hazard ratio (HR) associations, with acrolein showing the highest HR. The association between one interquartile range increase in acrolein exposure and breast cancer risk produced an adjusted HR of 2.26 (95% confidence interval: 1.92–2.65). The Cox proportional hazards models were adjusted for various covariates (e.g., race/ethnicity, BMI, physical activity, hormone replacement therapy, relative history of breast cancer, and age at menarche). Among traffic-related pollutants, higher HRs for acrolein were observed in African Americans and Whites compared to other racial and ethnic groups (p-heterogeneity <0.05). The study had several strengths, including a large sample size, a prospective cohort design, time to event analysis, and a racially/ethnically diverse multiethnic population. It also utilized comprehensive questionnaires that captured a wide range of covariates, along with detailed residential histories for participants living in California during the study period. The analysis was well-powered to examine air toxics, given its urban setting with elevated levels of traffic and industrial pollution. A notable feature was the inclusion of neighborhoods predominantly composed of historically marginalized racial and ethnic groups, who have experienced disproportionate pollution exposure.

However, interpretation of the acrolein results was constrained by potential collinearity with other air toxics (1,3-butadiene, toluene, ethylbenzene, acetaldehyde, and formaldehyde), which also showed significant associations with elevated breast cancer risk. Other limitations of this study include some imprecision and uncertainty in the NATA modeled air toxics exposure estimates at the census tract level, the non-exhaustive list of chemicals assessed (it is possible the chemicals studied are correlated with unmeasured chemicals) and the inability to account for exposures occurring earlier, outside of the study period.

Considering all the available epidemiologic studies, Etemadi et al. (2024) and Heck et al. (2024) provide some information on the carcinogenicity of acrolein. Overall, the evidence from epidemiology studies is still inadequate.

Toxicokinetics

The toxicokinetic information for acrolein has been reviewed extensively in recent reports by IARC (2021) and the Agency for Toxic Substances and Disease Registry (ATSDR, 2025).

Much of the toxicokinetic data relies on studies in rodents (Parent et al., 1996; Parent et al., 1998). Due to its high toxicity, no contolled human inhalation studies have been conducted that examine the metabolism of acrolein. Studies of acrolein urinary metabolites in humans have been conducted in smokers and in individuals following consumption of fried food (Hikisz & Jacenik, 2023a; 2023b).

An overview of the absorption, distribution, metabolism, and excretion of inhaled acrolein is described below:

- The electrophilic site of acrolein can react directly with the cysteinyl thiol (-SH) of proteins (lysine and histidine) and nonproteins (glutathione) and form covalent adducts with DNA (Esterbauer et al., 1975; Stevens & Maier, 2008).

- Due to acrolein's highly reactive electrophilicity, up to 98% uptake efficiency in the isolated upper respiratory tract (URT) occurred following inhalation exposure of anesthetized rats to 1.4 mg/m^3 (0.6 ppm) acrolein (Struve et al., 2008). Increasing concentration, increasing air flow rate, or extending exposure time reduced URT uptake efficiency (Struve et al., 2008; Morris, 1996).

- Three-dimensional computational fluid dynamic modeling predicts nasal breathing in humans results in 2–2.5 times less nasal extraction than that predicted in the rat (Schroeter et al., 2008). Additionally, oral breathing by humans will deliver more acrolein to the lower respiratory tract.

- In male and female rats administered radiolabeled acrolein by gavage, 30–31% of the initial dose was expired as CO_2, 52–63% was excreted in the urine, and 12–15% was eliminated in the feces (Parent et al., 1996). Tissue concentrations seven days following gavage were minimal (<1%).

- In humans, S-(3-hydroxypropyl)-N-acetylcysteine (HPMA) and S-carboxyethyl-N-acetylcysteine (CEMA) are the main acrolein metabolites excreted in urine by non-smokers, with considerably higher levels of these metabolites found in urine of smokers (Alwis 2012, 2015; Carmella et al., 2007). Increased urinary levels of HPMA is also found in e-cigarette users (Chen et al., 2023).

- The elimination half-time of urinary HPMA levels in humans was 9–10 hours following consumption of fried food (Wang et al., 2019; Watzek et al., 2012). The urinary elimination half-time was about 12 hours for CEMA.

As outlined in Figure 1, metabolism of acrolein first involves glutathione conjugation (non-enzymatic or catalyzed by glutathione-S-transferase), which occurs primarily in the liver. The conjugate then undergoes enzymatic cleavage of the γ-glutamic acid and glycine residues, followed by N-acetylation of the subsequent cysteine conjugate to form S-(3-oxopropyl)-N-acetylcysteine (OPSG). OPSG is then converted to S-(3-hydroxypropyl)glutathione (HPSG) via aldo-keto reductase (AKR) with subsequent reduction through the mercapturic acid pathway to form HPMA, which is the main urinary metabolite found in both rodents and humans. OPSG may also be reduced by alcohol dehydrogenase to form HPSG. Alternatively, OPSG can be oxidized by aldehyde dehydrogenase to S-(2-carboxyethyl)glutathione (CESG), then reduced via the mercapturic acid pathway to produce CEMA, another common urinary metabolite.

Minor routes shown in Figure 1 include oxidation of acrolein by aldehyde dehydrogenase to acrylic acid. Hydrolysis of acrylic acid generates 3-hydroxpropionic acid (HPA) and can eventually be metabolized to carbon dioxide and water. Another minor pathway for acrolein metabolism is oxidation by cytochrome P450 to glycialdehyde[4], an unstable intermediate. Glycialdehyde can react with water and epoxide hydrolase (EH) to form glyceraldehyde. Glycialdehyde may also be conjugated with glutathione (GSH) and subsequently reduced through the mercapturic acid pathway (MAP) to generate the urinary metabolite N-acetyl-S-(2-carboxy-2-hydroxyethyl)-cysteine (CHEMA).

Human aldose reductase, a member of the AKR superfamily, has been shown to reduce acrolein to allyl alcohol (Kolb et al., 1994). As already discussed above, AKR can also reduce the acrolein-GSH conjugate OPSG to HPSG (Shen et al., 2011). OPSG may also be oxidized by a flavin-containing monooxygenase (FMO) to yield

[4] Glycialdehyde is currently listed as causing cancer under California's Proposition 65 (OEHHA, 1988). US EPA (1991) has identified glycialdehyde as a Class B2 carcinogen (probable human carcinogen) based on experimental animal carcinogenicity bioassays. IARC classified glycialdehyde as a Group 2B carcinogen (possibly carcinogenic to humans) based on sufficient evidence in experimental animals (IARC, 1999).

OPSG-S-oxide, which can release acrolein to form sulfenic acid (Metabolic pathway not shown in Figure 1; Stevens and Maier, 2008).

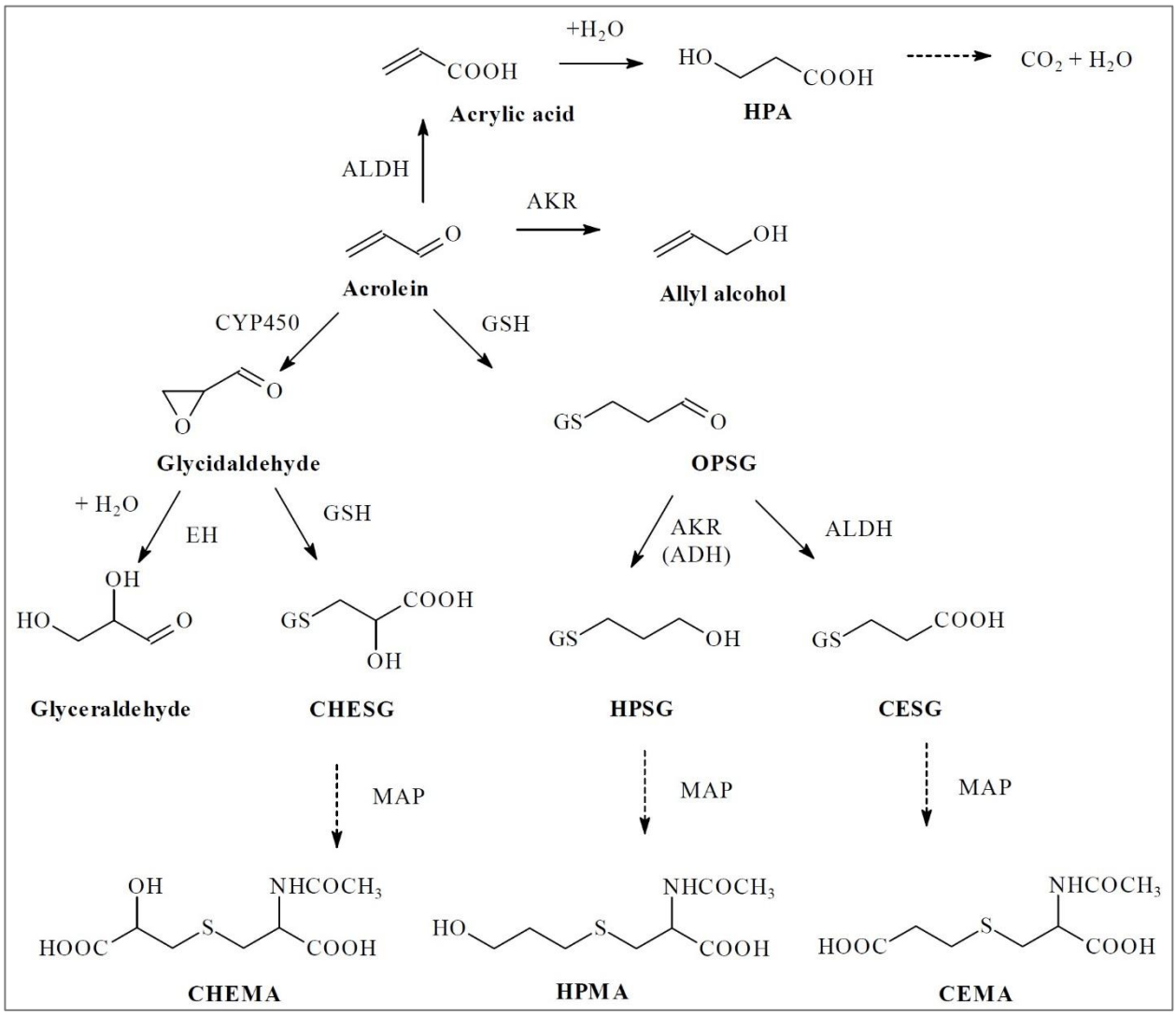

Figure 1. Metabolic Pathways of acrolein. Abbreviations: ADH – alcohol dehydrogenase; AKR – aldo-keto reductase; ALDH – aldehyde dehydrogenase; CEMA – N-acetyl-S-(carboxyethyl)-L-cysteine (2-carboxyethylmercapturic acid); CESG – S-(2-carboxyethyl)glutathione; CHEMA – N-acetyl-S-(2-carboxy-2-hydroxyethyl)-L-cysteine (2-carboxy-2-hydroxyethylmercapturic acid); CHESG – S-(2-carboxy-2-hydroxyethyl)glutathione; CYP450 – cytochrome P450; EH – epoxide hydrolase; GSH – glutathione; HPA – 3-hydroxypropanoic acid; HPMA – N-acetyl-S-(3-hydroxypropyl)-L-cysteine (3-hydroxypropylmercapturic acid); HPSG – S-(3-hydroxypropyl)glutathione; MAP – mercapturic acid pathway; OPSG – S-(3-oxopropyl)glutathione. Reproduced from IARC (2021), Figure 4.1.

Endogenous Formation

Small amounts of acrolein from both endogenous and exogenous sources have been detected in exhaled air (Andreoli et al., 2003; Ligor et al., 2008; Burcham, 2017). The median concentration of acrolein in exhaled breath condensate was 2.33 nanomolar (nM) in healthy nonsmokers (Andreoli et al., 2003). The median concentration in exhaled breath condensate in smokers was 6.78 nM, nearly three times higher than nonsmokers.

Polyamine degradation is thought to be the main endogenous source of acrolein (Igarashi & Kashiwagi, 2021). Spermine and spermidine are polyamines that are found in eukaryotic cells and are involved in regulating protein synthesis. Spermine oxidase-mediated degradation of these polyamines generates acrolein. The degradation of the amino acid threonine by myeloperoxidase in human neutrophils will also generate acrolein (Stevens & Maier, 2008; Hikisz & Jacenik, 2023a). Oxidation of unsaturated fatty acids by reactive oxygen species is another source of acrolein, which may be amplified during cellular stress (i.e., brain infarction, renal failure, and chronic inflammation). Under oxidative stress conditions, lipid peroxidation reactions proceed non-enzymatically on polyunsaturated fatty acids, including linoleic and α-linolenic acids, resulting in the generation of acrolein and other reactive carbonyl species (Moldogazieva et al., 2023).

In an exogenous vs. endogenous exposure assessment of acrolein by Rietjens et al. (2022), endogenous formation may outweigh exogenous exposure for people not heavily exposed to exogenous sources such as cigarette smoke, fried foods, or occupational acrolein emissions.

Nasal Dosimetry Models

Schroeter et al. (2008) developed three-dimensional computational fluid dynamic (CFD) models of rat and human nasal passages to estimate the inhaled acrolein tissue deposition throughout the nasal epithelium. In the rat model, a higher flux of acrolein into tissues in the anterior region of the nasal cavity was predicted compared to the posterior region. This finding was consistent with nasal tissue damage in the anterior region observed of rats exposed subchronically to acrolein. A human nasal CFD model was then used to extrapolate nasal extraction efficiency in rats to human exposure conditions. The calculated human acrolein nasal extraction at resting breathing conditions was consistently 2–2.5 times less than that predicted in the rat over an exposure concentration range of 0.6 to 3.6 ppm.

IARC (2021) notes that, because of oral breathing, delivery of acrolein to the lower respiratory tract could be higher in humans than in rats, which are obligate nasal

breathers. Thus, the delivery of acrolein to the lower respiratory tract will likely be higher in humans than in rats.

Asgharian et al. (2012) developed a human air-tissue transport model for lung uptake during a single breath for acrolein and other soluble, reactive gases. The model did not include vapor uptake in the upper respiratory tract. The rate of loss of inhaled acrolein from air to airway walls was greatest in airway branch generations 8–10 at rest but was greatest in airway branch generations 17–18 with heavy exercise.

Using molecular dynamic simulations and computational fluid dynamics with the rat nose model, Xi et al. (2017) demonstrated that the high polarity of inhaled acrolein leads to agglomeration of acrolein-acrolein and acrolein-water molecules in the respiratory tract. The agglomeration increased with higher acrolein concentrations, which reduced the effective gas diffusivity and led to lower deposition in the rat airway. Deposition in the nasal region was approximately 75–80% for droplet sizes <1 nm but decreased to approximately 20–30% for 8-nm droplets. Xi et al. suggests that molecular agglomeration in addition to reduced reaction rates (i.e., GSH depletion) both contribute to decreased diffusivity in the nose at higher acrolein concentrations.

Genotoxicity

Studies on the genotoxicity of acrolein have been comprehensively summarized by IARC (2021) and ATSDR (2025). These studies were conducted in various *in vitro* and *in vivo* systems, with and without metabolic activation.

IARC (2021) states the following regarding the body of literature for the genotoxicity of acrolein:

> "Acrolein is genotoxic. No data in humans in vivo were available. In several studies in human primary cells, acrolein consistently induced DNA strand breaks and DNA–protein crosslinks. In cultured human cell lines, acrolein consistently induced DNA strand breaks, mutations, and micronucleus formation, and was suggestive of inducing DNA–protein crosslinks. A limited number of in vivo studies of genotoxic endpoints were available and were largely negative; however, across many in vitro experimental systems acrolein was found to consistently induce DNA strand breaks, DNA–protein crosslinks, mutations, and sister-chromatid exchanges. In Salmonella strains tested without metabolic activation, acrolein induced both base-pair substitution and frameshift mutations. The mutagenicity of acrolein has also been demonstrated in experiments with plasmid DNA."

In addition, DNA binding studies in animal and human cells have been conducted both in vivo and in vitro. IARC (2021) states the following regarding the DNA binding evidence for acrolein:

> "Acrolein is a strongly electrophilic α,β-unsaturated aldehyde (enal) that readily reacts with DNA bases and proteins forming DNA and protein adducts in vivo and in vitro. Among these adducts, the most widely studied are the cyclic deoxyguanosine adducts, which are formed as a pair of α and γ regioisomers, α- and γ-hydroxy-1,N2-propano-2´-deoxyguanosine (α- and γ-OH-PdG, also known as α- and γ-OH-Acr-dGuo). γ-OH-PdG has been consistently detected in humans in various samples (including from lung, liver, brain, urothelial mucosa, and saliva), as well as in experimental animals, with detected levels dependent on species, tissue types, exposure, and physiological conditions."

In conclusion, regarding the overall mechanistic evidence for acrolein carcinogenicity, IARC (2021) stated that:

> "There is strong evidence that acrolein exhibits multiple key characteristics of carcinogens; acrolein is electrophilic; it is genotoxic; it alters DNA repair or causes genomic instability; it induces oxidative stress; it is immunosuppressive; it induces chronic inflammation; and it alters cell proliferation, cell death, or nutrient supply. The supporting data that acrolein exhibits these key characteristics comes primarily from studies with human primary cells and studies in experimental systems, and is supported by studies in humans for DNA adducts."

In the updated literature search since 2021, OEHHA identified four studies examining the relationship of acrolein-DNA adduct levels in oral/buccal cells of smokers and users of e-cigarettes (Table 4) and two studies examining formation of acrolein-DNA adducts *in vitro*.

Cheng et al. (2022) observed an increase in the acrolein-DNA adduct (8R/S-3)-(2'-deoxyribos-1'-yl)-5,6,7,8-tetrahydro-8-hydroxypyrimido[1,2-a]purine-10-(3H)-one (γ-OH-Acr-dGuo) in buccal cells of e-cigarette users compared to non-users of any tobacco or nicotine product. Although e-cigarettes lack tobacco leaves and combustion, heated e-cigarette vapor does contain numerous toxicants including acrolein. Participants visited the clinic once a month for oral sample collection. The average median value of γ-OH-Acr-dGuo in the DNA of buccal cells collected from three visits was 178.8 femtomole per micromole (fmol/μmol) γ-OH-Acr-dGuo for e-cigarette users and 21.0 fmol/μmol γ-OH-Acr-dGuo for non-users, a significant 9-fold difference (p = 0.001). The researchers also determined γ-OH-Acr-dGuo levels in buccal cells of eight cigarette smokers who provided samples during the first visit.

The median value was 446 fmol/μmol dGuo, which was significantly higher than that in e-cigarette users ($p < 0.001$).

In a cohort study of Chinese never-smokers (n = 40) and current smokers (n = 40) by Cheng et al. (2023), the number of γ-OH-Acr-dGuo adducts in buccal cell DNA was significantly higher ($p < 0.001$) in current smokers (90.5 adducts/10^9 nucleosides) compared to never smokers (7.2 adducts/10^9 nucleosides). In a case-control portion of the study, a cohort of 20 participants with lung cancer was matched with 20 participants without lung cancer. No significant association between buccal cell adduct levels and risk of lung cancer incidence was found (cases and controls were matched on smoking status).

Park et al. (2022) quantified the acrolein-DNA adduct γ-OH-Acr-dGuo and a lipid peroxidation-related adduct 1,N^6-etheno-dAdo (εdAdo) in oral cell DNA obtained from smokers among three ethnic groups: Native Hawaiians, Whites, and Japanese American adults living in Hawaii. After model adjustment for age, sex, log-total nicotine equivalents, log-HPMA, and race/ethnicity, Whites had significantly higher levels of γ-OH-Acr-dGuo than Japanese Americans and Native Hawaiians ($p < 0.05$); with geometric means of 64.4, 47.9 and 50.5 adducts per 10^9 nucleotides, respectively. Following the same model adjustment, higher levels of εdAdo were observed in Native Hawaiian versus Japanese American and White cigarette smokers ($p = 0.05$ or 0.06) suggesting increased lipid peroxidation may result in higher cancer risk for Native Hawaiian smokers.

Acrolein-DNA adducts were assessed in buccal cells of 213 tobacco smokers throughout the four phases of a 10-week study designed to test the effect of various interventions (substitution of usual brand cigarettes with very low nicotine content cigarettes with or without use of electronic cigarettes with high or low nicotine content; Robinson et al., 2025). The various interventions had no effect on an individual's buccal cell levels of acrolein-DNA adduct γ-OH-Acr-dGuo. The study made no measurements or estimates of changes in acrolein exposure during the various study interventions.

A study investigating the use of the acrolein-DNA adduct γ-OH-Acr-dGuo (expressed as γ-OHPdG in this study), as a prognostic biomarker for recurrence of hepatocellular carcinoma assessed the specificity of an anti-γ-OH-Acr-dGuo antibody by treating HepG2 cells with 50 μM or 100 μM acrolein for 5 hours (Aggarwal et al., 2024). A significant acrolein concentration-dependent increase in γ-OH-Acr-dGuo-positive staining was observed in treated cells compared to untreated cells in both the whole cell and the nucleus.

Hurley et al. (2024) assessed cytotoxicity and formation of DNA adducts in human colorectal adenocarcinoma (SW480) cells following treatment with acrolein directly or as a result of exposure to spermine, which undergoes intracellular oxidation to form acrolein. A concentration-dependent increase in levels of γ-OH-Acr-dGuo (expressed as *γ*−HO−Acr-dG in this study) and a depletion in glutathione levels were observed in SW480 cells treated directly with 50, 75, and 100 μM acrolein for 6 hours at 37°C compared to unexposed cells. Similarly, a concentration-dependent increase in levels of γ-OH-Acr-dGuo was observed in SW480 cells treated with 100−600 μM spermine for 6 h at 37°C.

Table 4. Acrolein-induced adducts in human smokers and e-cigarette users.

Biosample	Location, setting	Exposure level and number of exposed and controls	Adduct frequency and response	Comments	Reference
Buccal cells	Buccal brushings from e-cigarette users and non-users of any tobacco or nicotine products over three monthly visits, and cigarette smokers from one visit	e-Cigarette users (n = 20) Non-users (n = 20) Cigarette smokers (n = 8)	γ-OH-Acr-dGuo[a] median levels: 178.8 fmol/μmol for e-cigarette users 21.0 fmol/μmol for non-users 446 fmol/μmol for smokers	e-Cigarette users required to use e-cigarettes at least four times per week. $p = 0.001$ (e-cigarette users vs. non-users) $p < 0.001$ (e-cigarette users vs. cigarette smokers)	Cheng et al., 2022
Buccal cells	Buccal wash samples collected during one follow-up visit of the Shanghai Cohort Study	Never smokers (n = 40) Current smokers (n = 40 each)	γ-OH-Acr-dGuo[a] median levels: 7.2 adducts/10^9 nucleosides for non-smokers. 90.5 adducts/10^9 nucleosides for smokers	Case-control cohort of participants with lung cancer cases vs. controls (n = 20 each), no significant relationship of γ-OH-Acr-dGuo level to lung cancer risk was found.	Cheng et al., 2023

[(a)] γ-OH-Acr-dGuo - γ-hydroxy-1,N2-propano-2´-deoxyguanosine, a cyclic deoxyguanosine acrolein-DNA adduct

863 **Table 4. Acrolein-induced adducts in human smokers and e-cigarette users (continued).**

Biosample	Location, setting	Exposure level and number of exposed and controls	Adduct frequency and response	Comments	Reference
Buccal Cells	Buccal brushings collected from tobacco smokers at the end of each of four phases. The 4 phases included phase 1 (week 1): use of usual brand cigarette, phase 2 (weeks 2–4): very low nicotine content cigarettes (VLNCC), phase 3 (weeks 5–7), and phase 4 (weeks 8–10): VLNCC + electronic cigarettes with high or low nicotine content	Participants recruited from the Houston metropolitan area (n = 213)	No significant difference of different interventions on levels of γ-OH-Acr-dGuo[a].	All participants were smokers	Robinson et al., 2025
Oral cells	Single oral rinse samples collected from Native Hawaiian, White, and Japanese American cigarette smokers	Native Hawaiians (n = 101) Whites (n = 101) Japanese Americans (n = 79)	γ-OH-Acr-dGuo[a] levels in smokers: Whites > Japanese Americans = Native Hawaiians. εdAdo adduct levels in smokers: Whites = Native Hawaiians ≥ Japanese Americans	Lung cancer risk in cigarette smokers is highest in Native Hawaiians compared to Whites and Japanese Americans; association found for εdAdo levels and cancer risk but not for γ-OH-Acr-dGuo levels and cancer risk	Park et al., 2022

864 [(a)] γ-OH-Acr-dGuo - γ-hydroxy-1,N2-propano-2′-deoxyguanosine, a cyclic deoxyguanosine acrolein-DNA adduct

865

In the updated literature search, OEHHA identified eight genotoxicity or mutagenicity studies published subsequent to the literature considered in IARC (2021). These studies are summarized below and presented in Table 5.

In an *in vitro* study with human gastric epithelial cells (GES-1), human intestinal epithelial cells (Caco-2) and human umbilical vein endothelial cells (HUVEC), the terminal deoxynucleotidyl transferase-mediated dUTP nick end labelling (TUNEL) assay was used to detect DNA breakage by fluorescent labelling of free 3′ -hydroxyl termini, and the DAPI assay was used to detect nuclear condensation, also by fluorescent labeling (Zou et al., 2021). Following acrolein treatment, these assays showed DNA breakage and nuclear condensation in the range of 25 to 50 µmol/L in GES-1 and CACO-2 cells, and 5 to 10 µmol/L in HUVEC cells. The addition of serine or alanine to the medium tended to scavenge acrolein and reduce DNA damage.

Using human bronchial epithelial (BEAS-2B) cells, Liu et al. (2022b) examined the effects of acrolein on DNA damage, DNA damage response (DDR), and mitochondrial apoptosis *in vitro*. Cells were exposed to 20, 40, or 80 µM acrolein for 24 hours. Acrolein depleted intracellular GSH in a dose-dependent manner, while the generation of reactive oxygen species and the expression of 8-Oxo-2'-deoxyguanosine (8-OHdG), an oxidative DNA damage marker, increased in a dose-dependent manner. The effects were consistent with a dose-dependent increase in tail DNA% and Olive tail moment in the Comet assay, which are indicators of DNA fragmentation. Using a fluorescence technique, nuclear condensation of acrolein-treated cells increased with increasing dose indicating a change in nuclear morphology.

Liu et al. (2022b) also demonstrated that the resulting oxidative DNA damage caused by acrolein induced cell cycle arrest at the G2/M phase in the cells, which then activated the DDR as shown by increased expression of the Ataxia telangiectasia-mutated (ATM) and Rad-3-related (ATR)/Chk1 and ATM/Chk2 signaling pathways. The expression of γ-H2AX, the phosphorylated form of the histone H2AX and a marker of DNA double-strand breaks, also increased. Molecular docking analysis showed that the bonding energy of acrolein with DNA was -0.286 kcal/mol, indicating that the binding releases energy and is spontaneous. In further work by the authors, exposure of BEAS-2B cells to acrolein resulted in mitochondrial apoptosis[5] by inducing dose-dependent alterations in expression of key proteins. Significant increases in Bax and cleaved Caspase-3

[5] In mitochondria-mediated apoptosis, alterations in the expression of Bcl-2 family protein occurs, resulting in mitochondrial outer membrane permeabilization, which can lead to the release of cytochrome c from the intermembrane space of the mitochondria to the cytoplasm and consequently activates the caspases cascade and induces apoptosis (Xiong et al., 2014).

expressions and a decrease in Bcl-2 expression were observed in acrolein-treated cells. In addition, there was a dose-dependent reduction in ATP content in acrolein-treated cells.

Using a similar methodology as that conducted by Liu et al. (2022b), Liu et al. (2022a) demonstrated that exposure of human umbilical vein endothelial cells (HUVECs) *in vitro* resulted in oxidative stress, activation of DDR, and mitochondrial apoptosis. Cells were exposed to acrolein concentrations of 12.5, 25, and 50 μM for 24 hours. HUVECs were used due to evidence that inhaled acrolein may impair the cardiovascular system by targeting vascular endothelial cells. Regarding the methods used to detect DNA damage, acrolein treatment increased expression of 8-OHdG, and fluorescence images of treated cells exhibited nuclear condensation and fragmentation with increasing dose of acrolein. Reactive oxygen species generation by acrolein induced G0/G1 phase arrest, which then promoted a dose-dependent expression of γ-H2AX, a marker of DNA double-strand breaks. Tsai et al. (2021) treated mouse fibroblast NIH/3T3 cells *in vitro* with acrolein (7.5 μM) for one month to determine its effect on oncogenic transformation. The treatment induced cell proliferation, anchorage-independent activity, spheroid formation ability and cell migration capacity in selected clones, indicating that acrolein can transform normal NIH/3T3 fibroblasts into malignant cells. Using the xenograft tumorigenicity assay a transformed NIH/3T3 cell clone was injected into nude mice, which resulted in tumor formation that was apparent at 10 days post-treatment. The authors also observed that acrolein induced cell proliferation, colony formation activity, and cell migration capacity in human normal colon epithelium CCD-841CoN. In both mouse and human cell models, complimentary DNA microarray with ingenuity pathway analysis showed that acrolein induced the RAS/MAPK signaling pathway. This pathway is known to contribute to colon carcinogenesis.

In another study, human gastric adenocarcinoma (AGS) cells were treated with acrolein, and an increase in immunostaining for γ-H2AX was observed compared to controls (McNamara et al., 2024). The γ-H2AX levels were significantly decreased in cells pretreated with 2-hydroxybenzylamine (2-HOBA), an electrophile scavenger, followed by exposure to acrolein, compared to cells exposed to acrolein only.

Ma et al. (2024) investigated the cytotoxicity and genotoxicity of e-cigarette aerosols on oral keratinocytes. Part of this study included assessment of acrolein since acrolein was detected in aerosols of commercial e-cigarettes. Protein levels of cleaved caspase-3 and γ-H2AX in normal oral keratinocyte spontaneously immortalized cell lysates were increased in response to treatment with 2.5 μg/ml acrolein (the maximum concentration tested) for 24 hours. Treatment with 2.5 μg/ml acrolein also led to a significant increase in cell death compared to untreated cells ($p < 0.0001$).

A study (Ashraf et al., 2025) investigated acrolein-induced cytotoxicity and DNA damage in immortalized human lung epithelial cells (BEAS-2B) under normal and hypoxic (low oxygen) conditions, and the role of hypoxia-inducible factor 1α (HIF-1α). HIF-1α is a transcription factor that regulates cell survival and angiogenesis in response to hypoxia. The study included silencing the HIF-1α gene in BEAS-2B cells using transfection with small interfering RNA designed to target HIF-1α (si-HIF1A). Treatment groups included unexposed BEAS-2B cells (untreated control), 40 μM acrolein-exposed BEAS-2B cells (acrolein only), unexposed si-HIF1A cells, and 40 μM acrolein-exposed si-HIF1A cells. Two oxygen conditions were applied to each treatment group: normal and hypoxic. Experiments in this study included assessing cytotoxicity using lactate dehydrogenase release, cell viability using MTT assay, DNA fragmentation using comet assay, and oxidative DNA damage using concentrations of 8-OHdG. Acrolein-exposed si-HIF1A cells showed significant increases in cytotoxicity compared to acrolein treated BEAS-2B cells ($p < 0.0001$ for normoxia conditions, $p < 0.05$ for hypoxia conditions). There were significant decreases in cell viability in acrolein-treated si-HIF1A cells compared to acrolein-treated normal BEAS-2B cells treated in both normal and hypoxic conditions ($p < 0.0001$). si-HIF-1α transfection alone did not reduce cell viability. DNA damage as measured by the Olive tail moment in comet assay was significantly increased in acrolein-exposed BEAS-2B cells compared to untreated controls in both oxygen conditions ($p < 0.05$). Additionally, Olive tail moment was significantly increased in acrolein - exposed si-HIF1A cells compared to acrolein-exposed BEAS-2B cells in the hypoxia condition only, indicating the role of HIF-1α in decreasing acrolein-induced DNA damage ($p < 0.05$). There were no significant differences in 8-OHdG concentrations between various treatment groups, indicating an absence of oxidative DNA damage by acrolein in normal or hypoxic conditions. Overall, the results indicated that acrolein exposure decreased cell viability and increased DNA fragmentation. Silencing HIF-1α significantly increased these observed effects in hypoxic conditions.

Peterson et al. (2024) conducted a study to assess genotoxicity of acrolein using immortalized human (HT-1376 and T24) and canine (K9TCC-AxC and K9TCC-SH) urothelial cell lines, and primary human and canine urothelial cells. DNA damage was assessed by measuring tail DNA % using the comet assay and levels of γ-H2AX using immunocytochemistry. The canine cells were treated with a range of acrolein concentrations (0–55.6 μM). A significant increase in γ-H2AX and tail DNA % was observed in canine K9TCC-AxC urothelial cells treated with 55.6 μM acrolein compared to controls. Similarly, a significant increase in tail DNA % was observed in canine K9TCC-SH cells treated with 35.7 μM and 55.6 μM acrolein, while an increase in γ-H2AX was only observed at 35.7 μM acrolein. A concentration-dependent increase in tail DNA % was observed in canine primary urothelial cells treated with acrolein, with significant increases at 35.7, 46, and 55.6 μM. Human primary urothelial cells were more sensitive to acrolein-induced DNA damage compared to immortalized urothelial

cells. Significant increases in % DNA tail were observed in human primary urothelial cells at acrolein concentrations of ≥ 1.1 μM, and in HT-1376 and T24 cells at acrolein concentrations ≥ 2.1 μM and ≥ 2.9 μM, respectively. Levels of γ-H2AX were significantly increased in HT-1376 and T24 cells treated with acrolein concentrations ≥ 1.8 μM and ≥ 4.4 μM, respectively.

Table 5. Genetic and related effects of acrolein in human and animal cells (studies published after IARC, 2021).

Biological Endpoint	Cell Type or Species/Strain	Description	Result	Reference
DNA damage	Human GES-1 cells	TUNEL assay to detect DNA breakage	+[a] 25, 50 µmol/L	Zou et al., 2021
DNA damage	Human GES-1 cells	DAPI assay to detect nuclear condensation	+[a] 25, 50 µmol/L	Zou et al., 2021
DNA damage	Human Caco-2 cells	TUNEL assay to detect DNA breakage	+[a] 25, 50 µmol/L	Zou et al., 2021
DNA damage	Human Caco-2 cells	DAPI assay to detect nuclear condensation	+[a] 25, 50 µmol/L	Zou et al., 2021
DNA damage	Human HUVEC cells	TUNEL assay to detect DNA breakage	+[a] 5, 10 µmol/L	Zou et al., 2021
DNA damage	Human HUVEC cells	DAPI assay to detect nuclear condensation	+[a] 5, 10 µmol/L	Zou et al., 2021
Oxidative DNA damage	Human BEAS-2B cells	Expression of 8-OHdG	+ 20**, 40**, 80** µM	Liu et al., 2022b
DNA damage	Human BEAS-2B cells	Expression of γ-H2AX (indicator of double-strand breaks)	+ 20**, 40**, 80** µM	Liu et al., 2022b

Plus sign (+) – positive; NS – not significant; * *p*-value < 0.05. ** *p*-value < 0.01. *** *p*-value < 0.001. **** *p*-value < 0.00001
Abbreviations: AGS cells – human gastric adenocarcinoma cells; GES-1 – human gastric epithelial cells; HUVEC – human umbilical vein endothelial cells; NOKSI cells – Normal oral keratinocyte spontaneously immortalized cells; Caco-2 – human intestinal epithelial cells; TUNEL – Terminal deoxynucleotidyl transferase-mediated dUTP nick end labelling assay; DDR – DNA damage response; NIH/3T3 – mouse fibroblast cells; BEAS-2B – human bronchial epithelial cells, 8-OHdG: 8-Oxo-2'-deoxyguanosine, γ-H2AX: the phosphorylated form of the histone H2AX
[a] Statistical analysis not available

Table 5. Genetic and related effects of acrolein in human and animal cells (studies published after IARC, 2021; continued).

Biological Endpoint	Cell Type or Species/Strain	Description	Result	Reference
DNA damage	Human BEAS-2B cells	Tail DNA% (Comet assay)	+ 20**, 40**, 80** µM	Liu et al., 2022b
DNA damage	Human BEAS-2B cells	Olive tail moment (Comet assay)	+ 20*, 40**, 80** µM	Liu et al., 2022b
DNA damage	Human BEAS-2B cells	Nuclear condensation (fluorescence technique)	+ 20**, 40**, 80** µM	Liu et al., 2022b
Oxidative DNA damage	Human HUVEC cells	Expression of 8-OHdG	+ 12.5**, 25**, 50** µM	Liu et al., 2022a
DNA damage	Human HUVEC cells	Expression of γ-H2AX (indicator of double-strand breaks)	+ 12.5**, 25**, 50** µM	Liu et al., 2022a
DNA damage	Human HUVEC cells	Nuclear condensation (fluorescence technique)	+ 12.5**, 25**, 50** µM	Liu et al., 2022a
DNA damage	Human primary urothelial cells	Tail DNA% (Comet assay)	NS 0.5 µM + 1.1**, 2.1****, 3.6****, 4.4**** µM	Peterson et al., 2024

Plus sign (+) – positive; NS – not significant;* *p*-value < 0.05. ** *p*-value < 0.01. *** *p*-value < 0.001. **** *p*-value < 0.0001
Abbreviations: AGS cells – human gastric adenocarcinoma cells, Caco-2 – human intestinal epithelial cells; GES-1 – human gastric epithelial cells; HUVEC – human umbilical vein endothelial cells; TUNEL – Terminal deoxynucleotidyl transferase-mediated dUTP nick end labelling assay; DDR – DNA damage response; NIH/3T3 – mouse fibroblast cells; BEAS-2B – human bronchial epithelial cells, 8-OHdG: 8-Oxo-2'-deoxyguanosine, γ-H2AX: the phosphorylated form of the histone H2AX.
[a] Statistical analysis not available

Table 5. Genetic and related effects of acrolein in human and animal cells (studies published after IARC, 2021; continued).

Biological Endpoint	Cell Type or Species/Strain	Description	Result	Reference
DNA damage	Canine primary urothelial cells	Tail DNA% (Comet assay)	+ 20**, 35.7**, 46**, 55.6** µM	Peterson et al., 2024
DNA damage	Human urothelial cell line HT1376	Tail DNA% (Comet assay)	NS 0.4, 1.4 µM + 2.1**, 2.9**, 3.6**, 4.4**** µM	Peterson et al., 2024
DNA damage	Human urothelial cell line T24	Tail DNA% (Comet assay)	NS 0.4, 1.4, 2.1 µM + 2.9**, 3.6****, 4.4**** µM	Peterson et al., 2024
DNA damage	Canine urothelial cell line K9TCC AxC	Tail DNA% (Comet assay)	NS 4.5, 8.9, 13.4, 17.8, 35.7 µM + 55.6**** µM	Peterson et al., 2024
DNA damage	Canine urothelial cell line K9TCC SH	Tail DNA% (Comet assay)	NS 4.5, 8.9, 13.4, 17.8µM + 35.7**, 55.6** µM	Peterson et al., 2024

Plus sign (+) – positive; NS – not significant;* *p*-value < 0.05. ** *p*-value < 0.01. *** *p*-value < 0.001. *** *p*-value < 0.0001
Abbreviations: AGS cells – human gastric adenocarcinoma cells; Caco-2 – human intestinal epithelial cells; GES-1 – human gastric epithelial cells; HUVEC – human umbilical vein endothelial cells; NOKSI cells – Normal oral keratinocyte spontaneously immortalized cells; TUNEL – Terminal deoxynucleotidyl transferase-mediated dUTP nick end labelling assay; DDR – DNA damage response; NIH/3T3 – mouse fibroblast cells; BEAS-2B – human bronchial epithelial cells; 8-OHdG - 8-Oxo-2'-deoxyguanosin;, γ-H2AX - the phosphorylated form of the histone H2AX
[a] Statistical analysis not available

Table 5. Genetic and related effects of acrolein in human and animal cells (studies published after IARC, 2021; continued).

Biological Endpoint	Cell Type or Species/Strain	Description	Result	Reference
DNA damage	Human urothelial cell line HT1376	Immunostaining of γ-H2AX (indicator of double-strand breaks)	NS 0.4, 0.7, 1.1, 1.4 µM + 1.8*** ,2.1***, 2.9***, 3.6***, 4.4*** µM	Peterson et al., 2024
DNA damage	Human urothelial cell line T24	Immunostaining of γ-H2AX	NS 1.4,2.1,2.9, 3.6 µM + 4.4** µM	Peterson et al., 2024
DNA damage	Canine urothelial cell line K9TCC SH	Immunostaining of γ-H2AX	NS 4.5, 8.9, 13.4, 17.8, 55.6 µM + 35.7** µM	Peterson et al., 2024
DNA damage	Canine urothelial cell line K9TCC AxC	Immunostaining of γ-H2AX	NS 4.5, 8.9, 13.4, 17.8, 35.7 µM + 55.6**** µM	Peterson et al., 2024

Plus sign (+) – positive; NS – not significant;* *p*-value < 0.05. ** *p*-value < 0.01. *** *p*-value < 0.001. **** *p*-value < 0.00001
Abbreviations: AGS cells –human gastric adenocarcinoma cells; GES-1 – human gastric epithelial cells; HUVEC – human umbilical vein endothelial cells; NOKSI cells – Normal oral keratinocyte spontaneously immortalized cells; Caco-2 – human intestinal epithelial cells; TUNEL – Terminal deoxynucleotidyl transferase-mediated dUTP nick end labelling assay; DDR – DNA damage response; NIH/3T3 – mouse fibroblast cells; BEAS-2B – human bronchial epithelial cells, 8-OHdG: 8-Oxo-2'-deoxyguanosine, γ-H2AX: the phosphorylated form of the histone H2AX
[a] Statistical analysis not available

Table 5. Genetic and related effects of acrolein in human and animal cells (studies published after IARC, 2021; continued).

Biological Endpoint	Cell Type or Species/Strain	Description	Result	Reference
DNA damage	Human AGS cells	Immunostaining of γ-H2AX	+ 10**** µM	McNamara et al., 2025
DNA damage	NOKSI cells	Expression of γ-H2AX	+ 2.5 µM	Ma et al., 2025
DNA damage	Human BEAS-2B	Olive tail moment (Comet assay)	+ 40* µM	Ashraf et al. 2025
DNA damage	Human BEAS-2B	Levels of 8-OHdG	NS 40 µM	Ashraf et al. 2025
Oncogenic Transformation	Mouse fibroblast NIH/3T3 cells	Cell proliferation, anchorage-independent activity, spheroid formation ability and cell migration capacity	+ 7.5 µM*	Tsai et al., 2021
Oncogenic Transformation *in vivo*	Transformed mouse NIH/3T3 cell clones, nude mice	Tumor xenograft formation in nude mice injected with NIH/3T3 cell clones	+ 7.5 µM* Acrolein used to transform NIH/3T3 cells	Tsai et al., 2021

Plus sign (+) – positive; NS – not significant;* *p*-value < 0.05. ** *p*-value < 0.01. *** *p*-value < 0.001. **** *p*-value < 0.00001
Abbreviations: AGS cells – human gastric adenocarcinoma cells; GES-1 – human gastric epithelial cells; HUVEC – human umbilical vein endothelial cells; NOKSI cells – Normal oral keratinocyte spontaneously immortalized cells; Caco-2 – human intestinal epithelial cells; TUNEL – Terminal deoxynucleotidyl transferase-mediated dUTP nick end labelling assay; DDR – DNA damage response; NIH/3T3 – mouse fibroblast cells; BEAS-2B – human bronchial epithelial cells, 8-OHdG: 8-Oxo-2'-deoxyguanosine, γ-H2AX: the phosphorylated form of the histone H2AX
[a] Statistical analysis not available

V. CANCER HAZARD EVALUATION

OEHHA's evaluations of the carcinogenicity and genotoxicity data of acrolein are aligned with the conclusion by IARC (2021) that acrolein is "probably carcinogenic to humans" (a Group 2A carcinogen) based on sufficient evidence in experimental animals and strong mechanistic evidence.

Specifically, IARC (2021) found strong evidence that acrolein exhibits multiple key characteristics of carcinogens. These key characteristics include electrophilicity; genotoxicity; altering of DNA repair or causes genomic instability; induction of oxidative stress; immunosuppressive capability; induction of chronic inflammation; and altering cell proliferation, cell death, or nutrient supply.

VI. QUANTITATIVE CANCER RISK ASSESSMENT

In this section, OEHHA presents the rationale and computations used to estimate the cancer potency[6] of acrolein in humans using dose-response information from studies conducted with mice and rats.

Primary Data Sets for Analysis

While the Etemadi et al. (2024) and Heck et al. (2024) studies provided some information on the carcinogenic hazard of acrolein, they were not suitable for dose-response assessment. The inhalation carcinogenicity studies in male and female rats and mice by Matsumoto et al. (2021) were of sufficient quality for the dose-response analysis. In these rodent bioassays, significantly increased tumors were found at multiple sites in female mice and at one site in female rats. A rare tumor was found in the nasal cavity of one male rat and was considered treatment-related but was of such low incidence that dose-response analysis was not performed.

Dose-Response Model

Based on the toxicological information presented in the preceding sections, OEHHA determined that acrolein's likely mode of carcinogenic action is via genotoxicity. For this assessment, OEHHA used the multistage cancer model and adopted the linear low-

[6] OEHHA's cancer potency estimates are presented as Cancer Slope Factors in units of risk per milligram of chemical per kilogram body weight per day $((mg/kg\text{-}d)^{-1})$ and as Inhalation Unit Risk Factors in units of risk per microgram per cubic meter $((\mu g/m^3)^{-1})$.

dose hypothesis, as recommended by OEHHA's 2009 cancer risk assessment guidelines and implemented in US EPA's benchmark dose software (BMDS).[7]

Dose Calculations for Mice and Rats

For female rats, the acrolein chamber concentrations of 0, 0.1, 0.5, and 2 ppm were time-adjusted and converted to mg/m^3. Time adjustment is carried out to convert the intermittent chamber exposure conditions to continuous exposure over the life span of the animals (i.e., to simulate an annualized average air concentration).

$$C = \text{Chamber concentration (ppm)} \times \frac{2.29\ \text{mg/m}^3}{1\ \text{ppm}} \times \frac{6\ \text{hrs}}{24\ \text{hrs}} \times \frac{5\ \text{days}}{7\ \text{days}} \times \frac{\text{weeks on study}}{104\ \text{weeks}}$$

Where C = Time-adjusted acrolein concentration (mg/m^3).

Compared to the control group, a lower survival rate was observed in 2 ppm female rats. However, the lower survival rate did not occur until late in the study (after week 90), so a time-to-tumor modeling adjustment was not applied. The time-adjusted concentrations were 0, 0.0409, 0.204, and 0.818 mg/m^3, respectively (Table 6).

For the female mice, the acrolein chamber concentrations were 0, 0.1, 0.4, and 1.6 ppm, and they were 99 weeks on study. The time-adjusted concentrations were 0, 0.0389, 0.156, and 0.623 mg/m^3, respectively (Table 6).

The lifetime average daily dose, in mg/kg-d, is used for calculating the cancer potencies (Table 6). The time-weighted average body weight throughout the study is used to determine the inhalation rate (IR) to calculate the daily dose. The weighted average lifetime body weights for the female rat and mouse control groups were calculated based on the regular reporting of group mean body weights during the exposure periods (JBRC, 2016a,b). The time-weighted average body weights were 0.222 and 0.0284 kg for the control female rats and mice, respectively.

The formulas to calculate the IR based on rodent body weight reflect proportional differences of body weight (BW$^{2/3}$) on the respiratory rate within a species. The IR for female rats was determined using Equation 6.1a by OEHHA (2018b).

$$\text{Rats: IR (m}^3\text{/day)} = 0.702\ \text{m}^3\text{/day-kg} \times (\text{BW})^{2/3} \quad \text{Equation 6.1a}$$

[7] The linear low-dose hypothesis asserts that the incremental risk of exposure to a carcinogen increases in direct (linear) proportion to the long-term average daily dose of the substance. Thus, any amount of exposure greater than zero produces some amount of extra cancer risk.

Where: IR = Inhalation rate (m^3/day)

BW = Time-weighted average body weight (kg)

The IR for mice was determined using Equation 6.1b by Anderson (1983)

$$\text{Mice: IR } (m^3/\text{day}) = 0.0345\ m^3/\text{day} \times (BW \div 0.025)^{2/3} \quad \text{Equation 6.1b}$$

Where: IR = Inhalation rate (m^3/day)

BW = Time-weighted average body weight (kg)

The calculated daily IRs for female rats and mice were 0.257 and 0.0376 m^3/day, respectively.

The lifetime average daily doses for male and female mice and rats (shown in Table 6) were calculated using the following equation.

$$\text{Dose (mg/kg BW-day)} = IR \times C \div BW$$

Where C = time-adjusted acrolein concentration (mg/m^3).

Table 6. Calculated average daily dose of acrolein in female rats and mice.

Species	Chamber Concentration	Time-adjusted Concentration (mg/m^3)	Average daily dose (mg/kg-d)
Rats	0 mg/m^3, 0 ppm	0	0
	0.2 mg/m^3, 0.1 ppm	0.0409	0.047
	1.1 mg/m^3, 0.5 ppm	0.204	0.24
	0.9 mg/m^3, 0.4 ppm	0.818	0.95
Mice	0 mg/m^3, 0 ppm	0	0
	0.2 mg/m^3, 0.1 ppm	0.0389	0.052
	0.9 mg/m^3, 0.4 ppm	0.156	0.21
	3.7 mg/m^3, 1.6 ppm	0.623	0.82

Abbreviations: mg/m^3 –milligrams per cubic meter; mg/kg-d – milligrams per kilogram of body weight per day; ppm – parts per million.

Benchmark Dose Calculations

US EPA's BMD guidelines and software (version 3.3.2) were used to perform the multistage cancer model calculations (US EPA, 2024). In the multistage model, cancer potency is estimated based on the following expression relating the lifetime probability of a tumor at a specific site (*p*) to dose (d):

$$p(d) = \beta_0 + (1 - \beta_0)\,(1 - \exp\,[-\,(\beta_1 d + \beta_2 d^2 + \ldots + \beta_j d^j)])$$

In the above equation, “d” represents the average daily dose resulting from a uniform, continuous exposure over the nominal lifetime of the animal (two years for both rats and mice). When using a study in which the exposures vary in time, the exposures are averaged over the study period and modeled as uniform and continuous. The coefficients (β_0, β_1, etc.) are parameters estimated by fitting the data using maximum likelihood methods.

The overall incidence data in female rats and mice as presented in Tables 1 and 2 were used for cancer risk assessment. Individual animal survival data was not available to determine the effective tumor incidence. The effective tumor incidence is the number of

tumor-bearing animals (numerator) over the number of animals alive at the time of the first occurrence of the tumor (denominator) and is used to determine the cancer potency, when available.

BMD analyses were run for the female rat and mouse tumor data that were identified as treatment-related and showed a statistically significant increased incidence above control values and/or a statistically significant positive trend, using the average daily dose as presented in Table 6 as the dose metric. Tumors of the same histological cell type or tissue type were combined for dose-response assessment (McConnell et al., 1986; Brix et al., 2010).

For large datasets that contain 50 rodents/group/sex, a Benchmark Response (BMR) of 5% is recommended by OEHHA (2008) for the BMD and the 95% lower confidence bound (i.e., BMDL). First- and 2nd-degree multistage models were run for all suitable tumor data sets, and the most appropriate model fit was chosen based on BMD technical guidance (US EPA, 2022).

Acrolein induced a significant positive trend for rhabdomyomas in the nasal cavity in female rats, a rare tumor type in this rat strain. Combined incidences of rhabdomyomas and nasal squamous cell carcinomas were reported by JBRC (2016a) and Matsumoto et al. (2021) and used by the IARC (2021) evaluations even though they are of different histotypes. IARC (2021) considered the combined incidence of these two tumor types to be rare and treatment-related. Therefore, OEHHA modeled the combined incidences for these tumors as they were reported by the study authors and IARC (2021). In female mice, significant increases in trend and/or incidence for neoplasms at multiple sites were observed (nasal cavity adenomas and malignant lymphoma of the lymph nodes). In addition, in female mice a significant increase in the incidence of histiocytic sarcoma at the mid-dose was observed but considered as a finding that “may have been related to treatment” by IARC (2021) due to the lack of a clear dose-response relationship. Therefore, it is not clear that the histiocytic sarcomas of the uterus were treatment related, and only nasal cavity adenomas and malignant lymphoma of the lymph nodes were included in the dose-response analysis.

For female mice, the combined cancer potency was estimated using the multisite tumor module provided in BMDS. The BMDS procedure for summing risks over several tumor sites is based on the profile likelihood method. In this method, the maximum likelihood estimates for the multistage model parameters (β_i) for each tumor type are added together (i.e., $\sum\beta_0$, $\sum\beta_1$, $\sum\beta_2$, etc.), and the resulting model is used to determine a combined BMD. Then, a confidence interval for the combined BMD is calculated by computing the desired percentile of the chi-squared distribution associated with a likelihood ratio test having one degree of freedom.

Benchmark Dose Results

The BMDS modeling results for the female rat and mouse tumor data, including the BMD and BMDL values and adequacy measures related to the model fit, are presented in Table 7. CSFs in units of $(mg/kg\text{-}d)^{-1}$ were calculated as 0.05 ÷ BMDL, where 0.05 represents the 5% tumor response. Due to the high mortality observed in all exposure groups of female mice, the study was terminated at 99 weeks. An adjusted animal CSF_a was calculated to account for the short study duration and extrapolate to two years (104 weeks; OEHHA, 2009):

$$CSF_a = CSF_{a\text{-unadjusted}} \times (104 \text{ weeks}/\text{study duration})^3$$

Equivalent human CSFs (CSF_h) were calculated from animal CSFs (CSF_a) by multiplying the CSF_a by the ratio of human-to-animal body weights ($BW_h \div BW_a$) raised to the one-fourth power when animal potency is expressed in units of $(mg/kg\text{-}d)^{-1}$:

$$CSF_h = CSF_a \times (BW_h \div BW_a)^{1/4}$$

The body weights for mice and rats applied in the equation were the same values described above for the average daily dose calculation. The default body weight for humans is 70 kg (OEHHA, 2009). This interspecies scaling approach is used to account for differences between test animals and humans in pharmacokinetics (e.g., breathing rate, metabolism), and pharmacodynamics (e.g., tissue responses to chemical exposure) (US EPA, 2005).

The highest CSF_h resulted from the multisite tumor analysis in female mice. The multisite tumor CSF_h was 2.76 $(mg/kg\text{-}d)^{-1}$. The graphed BMD results for nasal cavity adenomas and malignant lymphoma are shown in Attachment A.

Table 7. BMDS modeling results for female rats and mice from the acrolein inhalation carcinogenicity bioassays by Matsumoto et al. (2021).

Sex Species	Tumor Site	BMD (mg/kg-d)	BMDL (mg/kg-d)	Goodness-of-Fit *p*-value	Animal CSF $(mg/kg\text{-}d)^{-1}$	Human CSF $(mg/kg\text{-}d)^{-1}$
Female Rats	Nasal cavity: Squamous cell carcinoma (SCC)[a]	1.030765	0.685448	0.998	0.073	0.308
	Nasal cavity: Rhabdomyoma (R)	0.812492	0.517358	0.995	0.097	0.408
	Nasal Cavity: SCC & R	0.704719	0.443972	0.991	0.113	0.476
Female Mice	Nasal cavity: Adenoma	0.421449	0.278521	0.954	0.208[b]	1.47
	Lymph node: Malignant lymphoma	0.502487	0.154967	0.257	0.374[b]	2.64
	Multisite	0.361	0.148	NA	0.392[b]	2.76

Abbreviations: BMD – Benchmark Dose; BMDL – Benchmark Dose (Lower confidence level); BMDS – Benchmark Dose Software; CSF – cancer slope factor; mg/kg-d – milligrams per kilogram of body weight per day; NA – not applicable (value not available for modeling procedure); $(mg/kg\text{-}d)^{-1}$ – per milligram per kilogram of body weight per day.

(a) Due to low tumor incidence in the high exposure group (2 out of 50) BMD modeling resulted in the BMD (i.e., 5% tumor response) that was greater than the highest exposure concentration.

(b) Animal CSF values for female mice data have been adjusted for study duration (99 weeks compared to the standard 104 weeks).

Inhalation Unit Risk Factor

Based on the dose-response results, the multisite tumor CSF_h in female mice was chosen by OEHHA as the critical data set from which to derive the acrolein IUR.

The IUR describes the excess cancer risk associated with inhalation exposure to a concentration of 1 $\mu g/m^3$ and is derived from the CSF_h:

$$IUR = (CSF_h \times BR_h) \div (BW_h \times CF)$$

Where:

BR_h = mean human breathing rate (20 m^3/day)
BW_h = mean human body weight (70 kg)
CF = mg-to-µg conversion factor of 1000

Use of the equation above with the acrolein CSF_h of 2.76 $(mg/kg\text{-}d)^{-1}$ (rounded to 2.8 $(mg/kg\text{-}d)^{-1}$ for the final health assessment values) results in a calculated IUR of 7.9×10^{-4} $(\mu g/m^3)^{-1}$ [3.4×10^{-4} $(ppb)^{-1}$].

Besides acrolein, other gaseous aldehydes found in urban air pollution include formaldehyde and acetaldehyde. The OEHHA Hot Spots IURs for formaldehyde and acetaldehyde are 6.0×10^{-6} and 2.7×10^{-6} $(\mu g/m^3)^{-1}$, respectively (OEHHA, 2023). Thus, acrolein is a more potent aldehyde.

VII. REFERENCES

Aggarwal M, Kuo M, Zhu Z, Gould S, Zhang K, Johnson P, Beheshtian S, Kuhlman L, Zhao Z, Fang H, Kallakury B, Creswell K, Mueller S, Kroemer A, He AR, and Chung FL (2024). Detection of γ-OHPdG in circulating tumor cells of patients with hepatocellular carcinoma as a potential prognostic biomarker of recurrence. *Gastro Hep Adv* 3(6): 809–820. DOI: 10.1016/j.gastha.2024.04.006. Last accessed May 2026, from https://www.sciencedirect.com/science/article/pii/S2772572324000566/pdfft?md5=50cb3e3b51b5f51d8406eb2adfda4887&pid=1-s2.0-S2772572324000566-main.pdf

Alwis KU, Blount BC, Britt AS, Patel D, and Ashley DL (2012). Simultaneous analysis of 28 urinary VOC metabolites using ultra high performance liquid chromatography coupled with electrospray ionization tandem mass spectrometry (UPLC-ESI/MSMS). *Anal Chim Acta* 750: 152–160. DOI: 10.1016/j.aca.2012.04.009. Last accessed May 2026, from https://pmc.ncbi.nlm.nih.gov/articles/PMC11261307/pdf/nihms-2010144.pdf

Alwis KU, deCastro BR, Morrow JC, and Blount BC (2015). Acrolein exposure in U.S. tobacco smokers and non-tobacco users: [National Health and Nutrition Examination Study] NHANES 2005–2006. *Environ Health Perspect* 123(12): 1302–1308. DOI: 10.1289/ehp.1409251. Last accessed May 2026, from https://pmc.ncbi.nlm.nih.gov/articles/PMC4671235/pdf/ehp.1409251.pdf

Anderson EL (1983). Quantitative approaches in use to assess cancer risk. *Risk Analysis* 3(4): 277–295. DOI: 10.1111/j.1539-6924.1983.tb01396.x.

Andreoli R, Manini P, Corradi M, Mutti A, and Niessen WM (2003). Determination of patterns of biologically relevant aldehydes in exhaled breath condensate of healthy subjects by liquid chromatography/atmospheric chemical ionization tandem mass spectrometry. *Rapid Commun Mass Spectrom* 17(7):637–645. DOI: 10.1002/rcm.960. Last accessed May 2026, from https://pmc.ncbi.nlm.nih.gov/articles/PMC1455504/pdf/nihms9762.pdf

Asgharian B, Price OT, Schroeter JD, Kimbell JS, and Singal M (2012). A lung dosimetry model of vapor uptake and tissue disposition. *Inhal Toxicol* 24(3): 182–193. DOI: 10.3109/08958378.2012.654857. Last accessed May 2026, from https://www.researchgate.net/profile/Jeffry-Schroeter/publication/221865433_A_lung_dosimetry_model_of_vapor_uptake_and_tissue_disposition/links/0c96053c551f314355000000/A-lung-dosimetry-model-of-vapor-uptake-and-tissue-disposition.pdf?_tp=eyJjb250ZXh0Ijp7ImZpcnN0UGFnZSI6InB1YmxpY2F0aW9uIiwicGFnZSI6InB1YmxpY2F0aW9uIn19

1233 Ashraf A, Zechmann B, and Bruce E (2025). Hypoxia-inducible factor 1α modulates
1234 acrolein-induced cellular damage in bronchial epithelial cells. *Toxicol* 515.154158. DOI:
1235 10.1016/j.tox.2025.154158.

1236 ATSDR (2025). *Toxicological Profile for Acrolein*. Agency for Toxic Substances and
1237 Disease Registry (ATSDR), Atlanta, GA. US Department of Health and Human
1238 Services. Last assessed May 2026, from
1239 https://www.atsdr.cdc.gov/ToxProfiles/tp124.pdf

1240 Bittersohl G (1975). Epidemiological research on cancer risk by aldol and aliphatic
1241 aldehydes. *Environ Qual Saf* 4: 235–238.

1242 Brix AE, Hardisty JF, and McConnell EE (2010). “Combining neoplasms for evaluation
1243 of rodent carcinogenesis studies” in, *Cancer Risk Assessment*. C-H Hsu and T
1244 Stedeford eds. John Wiley & Sons, Inc. pp. 619–715.

1245 Burcham PC (2017). Acrolein and human disease: untangling the knotty exposure
1246 scenarios accompanying several diverse disorders. *Chem Res Toxicol* 30(1):145–161.
1247 DOI: 10.1021/acs.chemrestox.6b00310.

1248 Cahill TM (2014). Ambient acrolein concentrations in coastal, remote, and urban regions
1249 in California. *Environ Sci Technol* 48(15): 8507–8513. DOI: 10.1021/es5014533. Last
1250 accessed May 2026, from
1251 https://pubs.acs.org/doi/pdf/10.1021/es5014533?ref=article_openPDF

1252 CARB (1997). *Acrolein*. Toxic Air Contaminant Identification List Summaries. California
1253 Air Resources Board (CARB), Sacramento, CA. Last accessed May 2026, from
1254 https://ww2.arb.ca.gov/sites/default/files/classic/toxics/tac/factshts1997/acrolein.pdf

1255 CARB (2025a). *iADAM: Air Quality Data Statistics*. California Air Resources Board
1256 (CARB), Sacramento, CA. Last accessed May 2026, from https://www.arb.ca.gov/adam

1257 CARB (2025b). *Study of Neighborhood Air near Petroleum Sources (SNAPS) Lost Hills,*
1258 *California*. *Final Report*. October 2025. California Air Resources Board (CARB),
1259 Sacramento, CA. Last accessed May 2026, from
1260 https://ww2.arb.ca.gov/sites/default/files/2025-10/SNAPS_Lost_Hills_Final_Report.pdf

1261

Carmella SG, Chen M, Zhang MY, Zhang S, Hatsukami DK, and Hecht SS (2007). Quantitation of acrolein-derived (3-hydroxypropyl)mercapturic acid in human urine by liquid chromatography-atmospheric pressure chemical ionization tandem mass spectrometry: effects of cigarette smoking. *Chem Res Toxicol* 20(7): 986–990. DOI: 10.1021/tx700075y. Last accessed May 2026, from https://pmc.ncbi.nlm.nih.gov/articles/PMC2556963/pdf/nihms59308.pdf

Chen M, Carmella SG, Lindgren BR, Luo X, Ikuemonisan J, Niesen B, Thomson NM, Murphy SE, Hatsukami DK, and Hecht SS (2023). Increased levels of the acrolein metabolite 3-hydroxypropyl mercapturic acid in the urine of e-cigarette users. *Chem Res Toxicol* 36(4): 583–588. DOI: 10.1021/acs.chemrestox.2c00145. Last accessed May 2026, from https://pmc.ncbi.nlm.nih.gov/articles/PMC9852357/pdf/nihms-1846935.pdf

Cheng G, Guo J, Carmella SG, Lindgren B, Ikuemonisan J, Niesen B, Jensen J, Hatsukami DK, Balbo S, and Hecht SS (2022). Increased acrolein-DNA adducts in buccal brushings of e-cigarette users. *Carcinogenesis* 43(5): 437–444. DOI: 10.1093/carcin/bgac026. Last accessed May 2026, from https://pmc.ncbi.nlm.nih.gov/articles/PMC9167028/pdf/bgac026.pdf

Cheng G, Guo J, Wang R, Yuan JM, Balbo S, and Hecht SS (2023). Quantitation by liquid chromatography-nanoelectrospray ionization-high-resolution tandem mass spectrometry of multiple DNA adducts related to cigarette smoking in oral cells in the Shanghai cohort study. *Chem Res Toxicol* 36(2): 305–312. DOI: 10.1021/acs.chemrestox.2c00393. Last accessed May 2026, from https://pmc.ncbi.nlm.nih.gov/articles/PMC10148603/pdf/nihms-1889162.pdf

DPR, 2021. *California Restricted Materials Requirement.* California Department of Pesticide Regulation (DPR), Sacramento, CA. Last accessed May 2026, from https://www.cdpr.ca.gov/wp-content/uploads/2024/08/dpr-enf-013a.pdf

DPR, 2022. *The Top Five Commodities by Pounds in each County in 2019 and the Top Five Chemicals used*. California Department of Pesticide Regulation (DPR), Sacramento, CA. Last accessed May 2026, from https://www.cdpr.ca.gov/wp-content/uploads/2024/12/2022_top_5_commodity_then_chemical_pounds_applied.pdf

DPR, 2024. *Active Ingredient: Acrolein. Human Health Risk Assessment and Mitigation. Documents and Activities*. California Department of Pesticide Regulation (DPR), Sacramento, CA. Last accessed May 2026, from https://www.cdpr.ca.gov/active-ingredient/acrolein/

Esterbauer H, Schaur RJ, and Zollner H (1991). Chemistry and biochemistry of 4-hydroxynonenal, malonaldehyde and related aldehydes. *Free Radic Biol Med* 11 (1): 81–128. DOI: 10.1016/0891-5849(91)90192-6. Last accessed May 2026, from https://www.researchgate.net/profile/Rudolf-Schaur/publication/223737675_Chemistry_and_biochemistry_of_4-hydroxynonenal_malonaldehyde_and_related_aldehydes/links/565c20e208ae1ef92981d432/Chemistry-and-biochemistry-of-4-hydroxynonenal-malonaldehyde-and-related-aldehydes.pdf?_tp=eyJjb250ZXh0Ijp7ImZpcnN0UGFnZSI6InB1YmxpY2F0aW9uIiwicGFnZSI6InB1YmxpY2F0aW9uIn19

Etemadi A, Poustchi H, Chang CM, Blount BC, Calafat AM, Wang L, De Jesus VR, Pourshams A, Shakeri R, Shiels MS, Inoue-Choi M, Ambrose BK, Christensen CH, Wang B, Murphy G, Ye X, Bhandari D, Feng J, Xia B, Sosnoff CS, Kamangar F, Brennan P, Boffetta P, Dawsey SM, Abnet CC, Malekzadeh R, and Freedman ND (2019). Urinary biomarkers of carcinogenic exposure among cigarette, waterpipe, and smokeless tobacco users and never users of tobacco in the Golestan Cohort Study. *Cancer Epidemiol Biomarkers Prev* 28 (2): 337–347. DOI: 10.1158/1055-9965. Last accessed May 2026, from https://pmc.ncbi.nlm.nih.gov/articles/PMC6935158/pdf/nihms-1063932.pdf

Etemadi AH, Poustchi CM, Chang AM, Calafat BC, Blount D, Bhandari, Wang L, Roshandel G, Alexandridis A, Botelho JC, Xia B, Wang Y, Sosnoff CS, Feng J, Nalini M, Khoshnia M, Pourshams A, Sotoudeh M, Gail MH, Dawsey SM, Kamangar F, Boffetta P, Brennan P, Abnet CC, Malekzadeh R, and Freedman ND (2024). Exposure to polycyclic aromatic hydrocarbons, volatile organic compounds, and tobacco-specific nitrosamines and incidence of esophageal cancer. *J Natl Cancer Inst* 116(3): 379–388. DOI: 10.1093/jnci/djad218. Last accessed May 2026, from https://pmc.ncbi.nlm.nih.gov/articles/PMC10919344/pdf/djad218.pdf

Faroon O, Roney N, Taylor J, Ashizawa A, Lumpkin MH, and Plewak DJ (2008). Acrolein environmental levels and potential for human exposure. *Toxicol Ind Health* 24: 543–564. DOI: 10.1177/0748233708098124.

Feng X, Qiu F, Zheng L, Zhang Y, Wang Y, Wang M, Xia H, Tang B, Yan C, and Liang R (2024). Exposure to volatile organic compounds and mortality in US adults: a population-based prospective cohort study. *Sci Total Environ* 928: 172512. DOI: 10.1016/j.scitotenv.2024.172512. Last accessed May 2026, from https://www.sciencedirect.com/science/article/pii/S0048969724026585/pdfft?md5=fa31f637c0eb09f0269d202615e974e4&pid=1-s2.0-S0048969724026585-main.pdf

Feron VJ and Kruysse A. (1977). Effects of exposure to acrolein vapor in hamsters simultaneously treated with benzo[a]pyrene or diethylnitrosamine. *J Toxicol Environ Health* 3(3): 379–394. DOI: 10.1080/15287397709529571.

Garcia-Gonzales DA, Shonkoff SBC, Hays J, and Jerrett M (2019). Hazardous air pollutants associated with upstream oil and natural gas development: a critical synthesis of current peer-reviewed literature. *Annu Rev Public Health* 40: 283–304. DOI: 10.1146/annurev-publhealth-040218-043715. Last accessed May 2026, from https://www.annualreviews.org/content/journals/10.1146/annurev-publhealth-040218-043715?crawler=true&mimetype=application/pdf

Ghilarducci DP and Tjeerdema RS (1995). Fate and effects of acrolein. *Rev Environ Contam Toxicol* 144: 95–146. DOI: 10.1007/978-1-4612-2550-8_2.

Heck JE, He D, Wing SE, Ritz B, Carey CD, Yang J, Stram DO, Le Marchand L, Park SL, Cheng I, and Wu AH (2024). Exposure to outdoor ambient air toxics and risk of breast cancer: the multiethnic cohort. *Int J Hyg Environ Health* 259: 114362. DOI: 10.1016/j.ijheh.2024.114362. Last accessed May 2026, from https://www.sciencedirect.com/science/article/pii/S1438463924000439/pdfft?md5=c655c9fe713f65ead4888d28636fb15d&pid=1-s2.0-S1438463924000439-main.pdf

Hikisz P and Jacenik D. (2023a). Diet as a source of acrolein: molecular basis of aldehyde biological activity in diabetes and digestive system diseases. *Int J Mol Sci* 24(7):6579. DOI: 10.3390/ijms24076579. Last accessed May 2026, from https://www.mdpi.com/1422-0067/24/7/6579/pdf?version=1680510788

Hikisz P and Jacenik D. (2023b). The tobacco smoke component, acrolein, as a major culprit in lung diseases and respiratory cancers: molecular mechanisms of acrolein cytotoxic activity. *Cells* 12(6): 879. DOI: 10.3390/cells12060879. Last accessed May 2026, from https://www.mdpi.com/2073-4409/12/6/879/pdf?version=1678528471

Hong JH, Lee PAH, Lu YC, Huang CY, Chen CH, Chiang CH, and Wang HT (2020). Acrolein contributes to urothelial carcinomas in patients with chronic kidney disease. *Urol Oncol* 38 (5): 465–475. DOI: 10.1016/j.urolonc.2020.02.017.

IARC (1995). “Acrolein” in, *IARC Monographs on the Evaluation of Carcinogenic Risks to Humans. Dry Cleaning, Some Chlorinated Solvents and Other Industrial Chemicals*. Volume 63. International Agency for Research on Cancer (IARC), Lyon, France. Last accessed May 2026, from https://publications.iarc.who.int/download/mono63.pdf

IARC (1999). *IARC Monographs on the Evaluation of Carcinogenic Risks to Humans. Re-Evaluation of Some Organic Chemicals, Hydrazine, and Hydrogen Peroxide.* Volume 71. International Agency for Research on Cancer (IARC), Lyon, France. Last accessed May 2026, from https://www.enviro.wiki/images/b/b4/IARC-1999_Monographs_Volume_71.pdf

IARC (2021). *IARC Monographs on the Identification of Carcinogenic Hazards to Humans. Acrolein, Crotonaldehyde, and Arecoline*. Volume 128. International Agency for Research on Cancer (IARC), Lyon, France. Last accessed May 2026, from https://publications.iarc.who.int/download/Volume128.pdf

Igarashi K and Kashiwagi K (2021). Functional roles of polyamines and their metabolite acrolein in eukaryotic cells. *Amino Acids* 53(10):1473–1492. DOI: 10.1007/s00726-021-03073-w.

JBRC (2016a). Summary of inhalation carcinogenicity study of acrolein in F344/DuCrlCrlj rats (tables). Hadano, Japan: Japan Bioassay Research Center (JBRC), Japan Industrial Safety and Health Association. Last accessed May 2026, from https://anzeninfo.mhlw.go.jp/user/anzen/kag/pdf/gan/0816TABLE.pdf

JBRC (2016b). Summary of inhalation carcinogenicity study of acrolein in B6D2F1/Crlj mice (tables). Hadano, Japan: Japan Bioassay Research Center (JBRC), Japan Industrial Safety and Health Association. Last accessed May 2026, from https://anzeninfo.mhlw.go.jp/user/anzen/kag/pdf/gan/0817TABLE.pdf

Jiang K, Huang C, Liu F, Zheng J, Ou J, Zhao D, and Ou S (2022). Origin and fate of acrolein in foods. *Foods* 11:1976. DOI: 10.3390/foods11131976. Last accessed May 2026, from https://www.mdpi.com/2304-8158/11/13/1976/pdf?version=1657163076

Hurley KA, Folz J, Zgraggen J, Cruz TN, Diedrich S, and Sturla SJ (2024). Enzymatic acrolein production system and its impact on human cells. *Chem Res Toxicol* 9;37(8): 1374–1381. DOI: 10.1021/acs.chemrestox.4c00119. Last accessed May 2026, from https://pmc.ncbi.nlm.nih.gov/articles/PMC11337209/pdf/tx4c00119.pdf

Kodell RL (2012). Should we assess tumorigenicity with the Peto or Poly-k Test? *Stat Biopharm Res* 4(2): 118–124. DOI: 10.1198/sbr.2010.10030.

Kolb NS, Hunsaker LA, and Vander Jagt DL (1994). Aldose reductase-catalyzed reduction of acrolein: implications in cyclophosphamide toxicity. *Mol Pharmacol* 45(4): 797–801.

Ligor T, Ligor M, Amann A, Ager C, Bachler M, Dzien A, and Buszewski B (2008). The analysis of healthy volunteers' exhaled breath by the use of solid-phase microextraction and GC-MS. *J Breath Res* 2(4):046006. DOI: 10.1088/1752-7155/2/4/046006.

Liu D, Cheng Y, Mei X, Xie Y, Tang Z, Liu J, and Cao X (2022a). Mechanisms of acrolein induces toxicity in human umbilical vein endothelial cells: oxidative stress, DNA damage response, and apoptosis. *Environ Toxicol* 37(4): 708–719. DOI: 10.1002/tox.23436.

Liu D, Cheng Y, Tang Z, Mei X, Cao X, and Liu J (2022b). Toxicity mechanism of acrolein on DNA damage and apoptosis in BEAS-2B cells: insights from cell biology and molecular docking analyses. *Toxicol* 466:153083. DOI: 10.1016/j.tox.2021.153083.

Ma T, Lee A, Eng B, Patel V, Michel SLJ, Kane MA, Dalby R, and Schneider A (2024). Aerosolized e-liquid base constituents induce cytotoxicity and genotoxicity in oral keratinocytes. *Oral Dis* 31(2): 482–491. DOI: 10.1111/odi.15104.

Marques MM, Beland FA, Lachenmeier DW, Phillips DH, Chung F-L, Dorman DC, Elmore SE, Hammond SK, Krstev S, Linhart I, Long AS, Mandrioli D, Ogawa K, Pappas JJ, Parra Morte JM, Talaska T, Tang M-S, Thakur N, van Tongeren M, Vineis P, Grosse Y, Benbrahim-Tallaa L, Suonio E, Turner MC, El Ghissassi F, Middleton D, Miranda-Filho A, Chung F, Liu Y, Vega S, Mattock H, Schubauer-Berigan MK, and Guyton KZ (2021). Carcinogenicity of acrolein, crotonaldehyde, and arecoline. *Lancet Oncol* 22(1): 19–20. DOI: 10.1016/S1470-2045(20)30727-0.

Matsumoto M, Yamano S, Senoh H, Umeda Y, Hirai S, Saito A, Kasai T, and Aiso S (2021). Carcinogenicity and chronic toxicity of acrolein in rats and mice by two-year inhalation study. *Regul Toxicol Pharmacol* 121:104863. DOI: 10.1016/j.yrtph.2021.104863.

McConnell EE, Solleveld HA, Swenberg JA, and Boorman GA (1986). Guidelines for combining neoplasms for evaluation of rodent carcinogenesis studies. *J Natl Cancer Inst* 76(2): 283–289.

McNamara KM, Sierra JC, Latour YL, Hawkins CV, Asim M, Williams KJ, Barry DP, Allaman MM, Zagol-Ikapitte I, Luis PB, Schneider C, Delgado AG, Piazuelo MB, Tyree RN, Carson KS, Choksi YA, Coburn LA, Gobert AP, and Wilson KT (2025). Spermine oxidase promotes Helicobacter pylori-mediated gastric carcinogenesis through acrolein production. *Oncogene* 44(5): 296–306. DOI: 10.1038/s41388-024-03218-7.

Moldogazieva NT, Zavadskiy SP, Astakhov DV, and Terentiev AA (2023). Lipid peroxidation: Reactive carbonyl species, protein/DNA adducts, and signaling switches in oxidative stress and cancer. *Biochem Biophys Res Commun* 687:149167. DOI: 10.1016/j.bbrc.2023.149167.

Morris JB (1996). Uptake of acrolein in the upper respiratory tract of the F344 rat. *Inhal Toxicol* 8(4): 387–403. DOI: 10.3109/08958379609052914

Nalini M, O'Brien KM, Calafat AM, Wang L, Feng J, Reese CM, Xia B, Botelho JC, Wang Y, Seyler T, Roh EJ, Tashakkori NA, Blakney A, Xu K, Gail MH, Blount BC, Chang CM, Abnet CC, Sandler DP, Freedman ND, and Etemadi A (2026). Tobacco-related urinary biomarkers and lung cancer risk in women, a case-cohort analysis. *J Natl Cancer Inst*. DOI: 10.1093/jnci/djag078.

NCBI (2024). *PubChem Compound Summary for CID 7847, Acrolein*. National Center for Biotechnology Information (NCBI). Last accessed May 2026, from https://pubchem.ncbi.nlm.nih.gov/compound/7847

NOAA (2024). *Acrolein, Stabilized.* CAMEO Chemicals database. National Oceanic and Atmospheric Administration (NOAA). Last accessed May 2026, from https://cameochemicals.noaa.gov/chemical/2300

OEHHA, 1988. *Glycialdehyde*. Office of Environmental Health Hazard Assessment (OEHHA). California Environmental Protection Agency, Sacramento, CA. Last accessed May 2026, from https://oehha.ca.gov/chemicals/glycidaldehyde

OEHHA (2008). *Air Toxics Hot Spots Program Risk Assessment Guidelines*. *Technical support document for the derivation of noncancer reference exposure levels*. Office of Environmental Health Hazard Assessment (OEHHA). California Environmental Protection Agency, Oakland, CA. Last accessed May 2026, from http://www.oehha.ca.gov/air/hot_spots/rels_dec2008.html

OEHHA (2009). *Air Toxics Hot Spots Program Risk Assessment Guidelines*. *Technical Support Document for Cancer Potency Factors: Methodologies for derivation, listing of available values, and adjustments to allow for early life stage exposures*. Office of Environmental Health Hazard Assessment (OEHHA). California Environmental Protection Agency. Last accessed May 2026, from http://oehha.ca.gov/air/crnr/technical-support-document-cancer-potency-factors-2009

OEHHA, 2014. *Acrolein*. Office of Environmental Health Hazard Assessment (OEHHA). California Environmental Protection Agency, Sacramento, CA. Last accessed May 2026, from https://oehha.ca.gov/chemicals/acrolein

OEHHA (2018a). *Gasoline-related air pollutants in California*. Trends in exposure and health risk 1996 to 2004. Office of Environmental Health Hazard Assessment (OEHHA). California Environmental Protection Agency, Sacramento, CA. Last accessed May 2026, from https://oehha.ca.gov/media/downloads/air/report/oehhagasolinereportjanuary2018final.pdf

OEHHA (2018b). *Calculation of rat breathing rate based on bodyweight*. Office of Environmental Health Hazard Assessment (OEHHA). California Environmental Protection Agency. Last accessed May 2026, from https://oehha.ca.gov/media/downloads/crnr/calcuratbreathingrate092818.pdf

OEHHA, 2019. *Analysis of Refinery Chemical Emissions and Health Effects.* Office of Environmental Health Hazard Assessment (OEHHA). California Environmental Protection Agency, Sacramento, CA. Last accessed May 2026, from https://oehha.ca.gov/sites/default/files/media/downloads/faqs/refinerychemicalsreport032019.pdf

OEHHA (2023). *Appendix A: Hot Spots Unit Risk and Cancer Potency Values*. Office of Environmental Health Hazard Assessment (OEHHA). California Environmental Protection Agency. Last updated January 2025. Online at https://oehha.ca.gov/media/downloads/crnr/appendixa.pdf

Ott MG, Teta MJ, and Greenberg HL (1989a). Lymphatic and hematopoietic tissue cancer in a chemical manufacturing environment. *Am J Ind Med* 16(6): 631–643. DOI: 10.1002/ajim.4700160603.

Ott MG, Teta MJ, and Greenberg HL (1989b). Assessment of exposure to chemicals in a complex work environment. *Am J Ind Med* 16(6): 617–630. DOI: 10.1002/ajim.4700160602.

Parent RA, Caravello HE, and Sharp DE (1996). Metabolism and distribution of [2,3-^{14}C]acrolein in Sprague-Dawley rats. *J Appl Toxicol* 16(5): 449–457. DOI: 10.1002/(SICI)1099-1263(199609)16:5<449::AID-JAT369>3.0.CO;2-9.

Parent RA, Paust DE, Schrimpf MK, Talaat RE, Doane RA, Caravello HE, Lee SJ, and Sharp DE (1998). Metabolism and distribution of [2,3-^{14}C]acrolein in Sprague-Dawley rats. II. Identification of urinary and fecal metabolites. *Toxicol Sci* 43(2): 110–120. DOI: 10.1006/toxs.1998.2462.

Park SL, Le Marchand L, Cheng G, Balbo S, Chen M, Carmella SG, Thomson NM, Lee Y, Patel YM, Stram DO, Jensen J, Hatsukami DK, Murphy SE, and Hecht SS (2022). Quantitation of DNA adducts resulting from acrolein exposure and lipid peroxidation in oral cells of cigarette smokers from three racial/ethnic groups with differing risks for lung cancer. *Chem Res Toxicol* 35(10): 1914–1922. DOI: 10.1021/acs.chemrestox.2c00171.

Peto R, Pike MC, Day NE, Gray RG, Lee PN, Parish S, Peto J, Richards S, and Wahrendorf J (1980). “Guidelines for simple, sensitive significance tests for carcinogenic effects in long-term animal experiments” in, *Long-term and short-term screening assays for carcinogens: A critical appraisal*. IARC Monograph on the Evaluation of the Carcinogenic Risk of Chemicals to Human's, Annex to Supplement 2. Geneva: World Health Organization. pp. 311–426.

Peterson HM, Holler JC, Boswell A, and Trepanier LA (2024). Urothelial genotoxicity of environmental chemicals detected in the urine of healthy dogs and their owners. *J Clin Transl Sci*. 24;8(1):e172. DOI: 10.1017/cts.2024.546. Last accessed May 2026, from https://pmc.ncbi.nlm.nih.gov/articles/PMC11604503/pdf/S2059866124005466a.pdf

Peterson HM, Richards KA, Borza T, Wiedmer AM, Jabbour MT, Knoedler MA, Mani E, Dahman C, and Trepanier LA (2025). Household arsenic and acrolein exposures and risk of urothelial cell carcinoma. *J Clin Trans Res* 11(3): 88–98. DOI: 10.36922/jctr.24.00065. Last accessed May 2026, from https://api-journal.accscience.com/journal/article/preview?id=4984

Rice RB, Boaggio K, Olson NE, Foley KM, Weaver CP, Sacks JD, McDow SR, Holder AL, and LeDuc SD (2023). Wildfires increase concentrations of hazardous air pollutants in downwind communities. *Environ Sci Technol* 57: 21235−21248. DOI: 10.1021/acs.est.3c04153. Last accessed May 2026, from https://pmc.ncbi.nlm.nih.gov/articles/PMC10862657/pdf/nihms-1951533.pdf

Rietjens I, Arand M, Bolt HM, Bourdoux S, Hartwig A, Hinrichsen N, Kalisch C, Mally A, Pellegrino G, Ribera D, Thatcher N, and Eisenbrand G (2022). The role of endogenous versus exogenous sources in the exposome of putative genotoxins and consequences for risk assessment. *Arch Toxicol* 96(5): 1297–1352. DOI: 10.1007/s00204-022-03242-0. Last accessed May 2026, from https://link.springer.com/content/pdf/10.1007/s00204-022-03242-0.pdf

Robinson JD, Cui Y, Kypriotakis G, Engelmann JM, Karam-Hage M, Minnix JA, Green CE, Shete S, Hatsukami DK, Donny EC, Murphy SE, Hecht SS, Eissenberg T, Wetter DW, and Cinciripini PM (2025). Evaluating the human abuse potential of concurrent use of electronic cigarettes and low nicotine cigarettes among adults who smoke. *Exp Clin Psychopharmacol*. 33(2): 133–144. DOI: 10.1037/pha0000749. Last accessed May 2026, from https://pmc.ncbi.nlm.nih.gov/articles/PMC11932771/pdf/nihms-2057641.pdf

Rodriguez VI, Mammadova J, Permuth JB, Luthra A, Pena L, Friedman M, Dam A, Cappelle S, Malafa MP, Hallmon C, Miranda C, and Mok SRS (2024). Elevated urinary levels of fungal and environmental toxins in patients with pancreatic ductal adenocarcinoma. *J Gastrointest Cancer* 56(1):4. DOI: 10.1007/s12029-024-01125-4. Last accessed May 2026, from https://link.springer.com/content/pdf/10.1007/s12029-024-01125-4.pdf

Schroeter JD, Kimbell JS, Gross EA, Willson GA, Dorman DC, Tan YM, and Clewell HJ (2008). Application of physiological computational fluid dynamics models to predict interspecies nasal dosimetry of inhaled acrolein. *Inhal Toxicol* 20(3): 227–243. DOI: 10.1080/08958370701864235.

Shen Y, Zhong L, Johnson S, and Cao D (2011). Human Aldo-Keto Reductases 1B1 and 1B10: a comparative study on their enzyme activity toward electrophilic carbonyl compounds. *Chem Biol Interact* 191(1–3): 192–198. DOI: 10.1016/j.cbi.2011.02.004. Last accessed May 2026, from https://pmc.ncbi.nlm.nih.gov/articles/PMC3103604/pdf/nihms283195.pdf

Shu L, Zhang L, and Yang B (2017). Exact statistical tests on comparing tumor incidence trend in transgenic mouse carcinogenicity studies. *Stat Biopharm Res* 9 (1): 44–51. DOI: 10.1080/19466315.2016.1191533.

Stevens JF and Maier CS (2008). Acrolein: sources, metabolism, and biomolecular interactions relevant to human health and disease. *Mol Nutr Food Res* 52(1): 7–25. DOI: 10.1002/mnfr.200700412. DOI: 10.1080/01926230252929990. Last accessed May 2026, from https://pmc.ncbi.nlm.nih.gov/articles/PMC2423340/pdf/nihms-48373.pdf

STP Working Group (2002). Statistical methods for carcinogenicity studies. *Toxicol Pathol* 30 (3): 403–414. Last accessed May 2026, from https://journals.sagepub.com/doi/pdf/10.1080/01926230252929990

Struve MF, Wong VA, Marshall MW, Kimbell JS, Schroeter JD, and Dorman DC (2008). Nasal uptake of inhaled acrolein in rats. *Inhal Toxicol* 20(3): 217–225. DOI: 10.1080/08958370701864219.

Tsai HC, Tsou HH, Lin CC, Chen SC, Cheng HW, Liu TY, Chen WS, Jiang JK, Yang SH, Chang SC, Teng HW, and Wang HT (2021). Acrolein contributes to human colorectal tumorigenesis through the activation of RAS-MAPK pathway. *Sci Rep* 11(1):12590. DOI: 10.1038/s41598-021-92035-z. Last accessed May 2026, from https://www.nature.com/articles/s41598-021-92035-z.pdf

Tsou HH, Hu CH, Liu JH, Liu CJ, Lee CH, Liu TY, and Wang HT (2019). Acrolein is involved in the synergistic potential of cigarette smoking- and betel quid chewing-related human oral cancer. *Cancer Epidemiol Biomarkers Prev* 28(5): 954–962. DOI: 10.1158/1055-9965.EPI-18-1033. Last accessed May 2026, from https://aacrjournals.org/cebp/article-pdf/28/5/954/2285791/954.pdf

US EPA (1991). *Glycidaldehyde; CASRN 765-34-4*. Integrated Risk Information System (IRIS), United States Environmental Protection Agency (US EPA). Last accessed May 2026, from https://iris.epa.gov/static/pdfs/0315_summary.pdf

US EPA (2005). *Guidelines for Carcinogen Risk Assessment*. Risk Assessment Forum, United States Environmental Protection Agency (US EPA). EPA/630/P-03/001F. March 2005. Last accessed May 2026, from https://www.epa.gov/sites/default/files/2013-09/documents/cancer_guidelines_final_3-25-05.pdf

US EPA, 2010. *Data Quality Evaluation Guidelines for Ambient Air Acrolein Measurements*. United States Environmental Protection Agency (US EPA). Last accessed May 2026, from http://www3.epa.gov/ttnamti1/files/ambient/airtox/20101217acroleindataqualityeval.pdf

US EPA (2012). *Benchmark Dose Technical Guidance*. United States Environmental Protection Agency. National Center for Environmental Assessment. Last accessed May 2026, from https://www.epa.gov/sites/default/files/2015-01/documents/benchmark_dose_guidance.pdf

US EPA (2022). *Benchmark Dose Software, BMDS Version 3.3 User Guide (Oct 2022)*. United States Environmental Protection Agency (US EPA). Last updated October 26, 2022. Last accessed May 2026, from https://assessments.epa.gov/bmds/document/&deid=353980

US EPA (2024). US EPA Benchmark Dose Software (BMDS) Version 3.3.2. National Center for Environmental Assessment. United States Environmental Protection Agency (US EPA). Last updated April 2026. Last accessed May 2026, from https://www.epa.gov/bmds

Wang TW, Liu JH, Tsou HH, Liu TY, and Wang HT (2019). Identification of acrolein metabolites in human buccal cells, blood, and urine after consumption of commercial fried food. *Food Sci Nutr* 7: 1668–1676. DOI: 10.1002/fsn3.1001. Last accessed May 2026, from https://pmc.ncbi.nlm.nih.gov/articles/PMC6526626/pdf/FSN3-7-1668.pdf

Watzek N, Scherbl D, Feld J, Berger F, Doroshyenko O, Fuhr U, Tomalik-Scharte D, Baum M, Eisenbrand G, and Richling E (2012). Profiling of mercapturic acids of acrolein and acrylamide in human urine after consumption of potato crisps. *Mol Nutr Food Res* 56(12): 1825–1837. DOI: 10.1002/mnfr.201200323.

Xi J, Hu Q, Zhao L, and Si XA (2017). Molecular binding contributes to concentration dependent acrolein deposition in rat upper airways: CFD and Molecular Dynamics Analyses. *Int Mol Sci* 19 (4):997. DOI:10.3390/ijms19040997. Last accessed May 2026, from https://pmc.ncbi.nlm.nih.gov/articles/PMC5979435/pdf/ijms-19-00997.pdf

Xiong S, Mu T, Wang G, and Jiang X (2014). Mitochondria-mediated apoptosis in mammals. *Protein Cell* 5(10):737–749. DOI: 10.1007/s13238-014-0089-1. Last accessed May 2026, from https://pmc.ncbi.nlm.nih.gov/articles/PMC4180462/pdf/13238_2014_Article_89.pdf

Yuan JM, Gao YT, Wang R, Chen M, Carmella SG, and Hecht SS (2012). Urinary levels of volatile organic carcinogen and toxicant biomarkers in relation to lung cancer development in smokers. *Carcinogenesis* 33(4): 804–809. DOI: 10.1093/carcin/bgs026. Last accessed May 2026, from https://pmc.ncbi.nlm.nih.gov/articles/PMC3384073/pdf/bgs026.pdf

Yuan JM, Butler L M, Gao YT, Murphy SE, Carmella SG, Wang R, Nelson HH, and Hecht SS (2014). Urinary metabolites of a polycyclic aromatic hydrocarbon and volatile organic compounds in relation to lung cancer development in lifelong never smokers in the Shanghai Cohort Study. *Carcinogenesis* 35(2): 339–345. DOI: 10.1093/carcin/bgt352. Last accessed May 2026, from https://pmc.ncbi.nlm.nih.gov/articles/PMC3908750/pdf/bgt352.pdf

Zou Z, Yin Z, Ou J, Zheng J, Liu F, Huang C, and Ou S (2021). Identification of adducts formed between acrolein and alanine or serine in fried potato crisps and the cytotoxicity-lowering effect of acrolein in three cell lines. *Food Chem* 361:130164. DOI: 10.1016/j.foodchem.2021.130164.

ATTACHMENT A

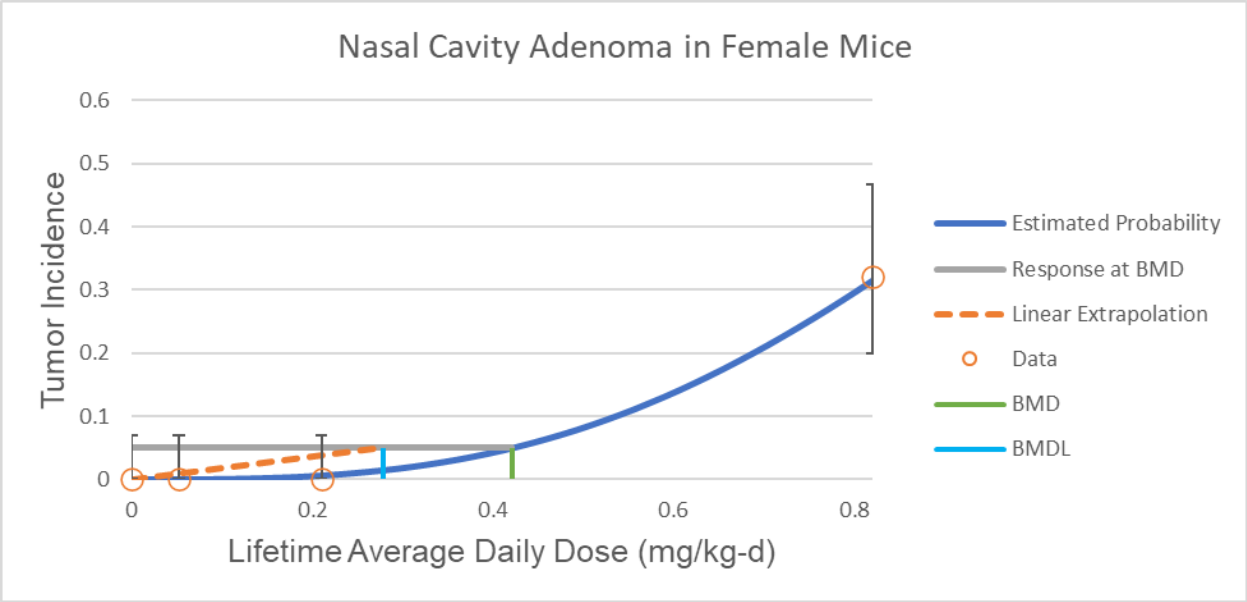

Figure A-1. Benchmark Dose results for nasal cavity adenoma in female mice. The Line graph shows the frequentist Multistage Degree 3 model with a benchmark response (BMR) of 5% extra risk for the benchmark dose (BMD) and 95% lower confidence limit for the benchmark dose (BMDL).

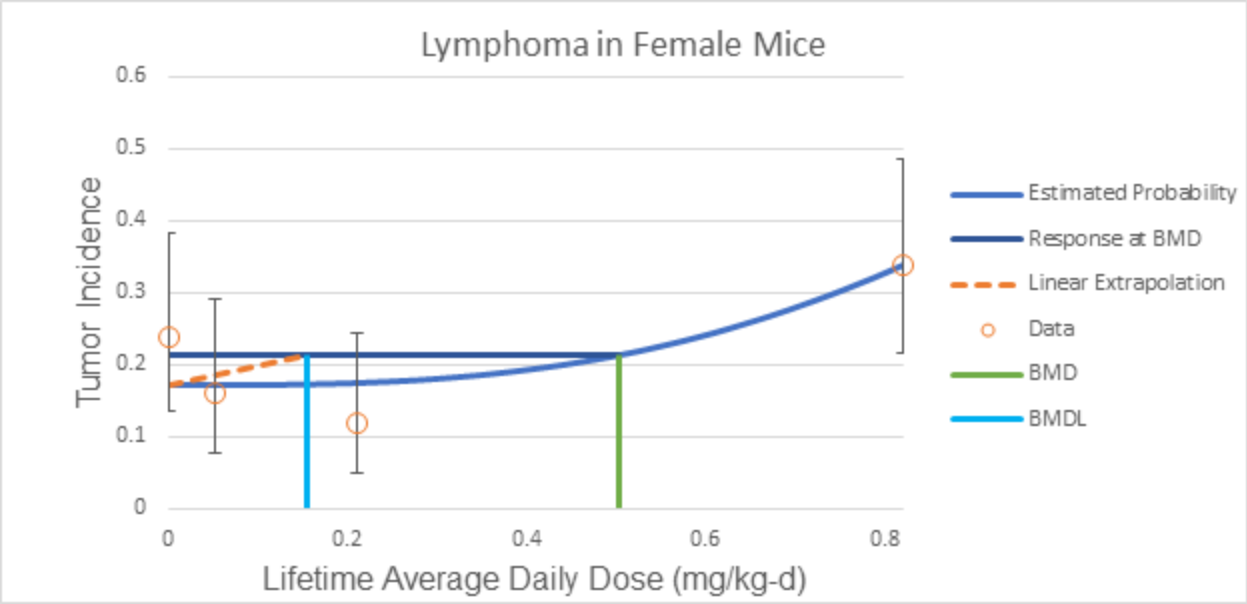

Figure A-2. Benchmark Dose results for lymphoma in female mice. The Line graph shows the frequentist Multistage Degree 3 model with a benchmark response (BMR) of 5% extra risk for the benchmark dose (BMD) and 95% lower confidence limit for the benchmark dose (BMDL).